Molecular BioSystems

Interfacing chemical biology with the -omic sciences and systems biology

www.molecularbiosystems.org

Volume 8 | Number 12 | December 2012 | Pages 3091–3348

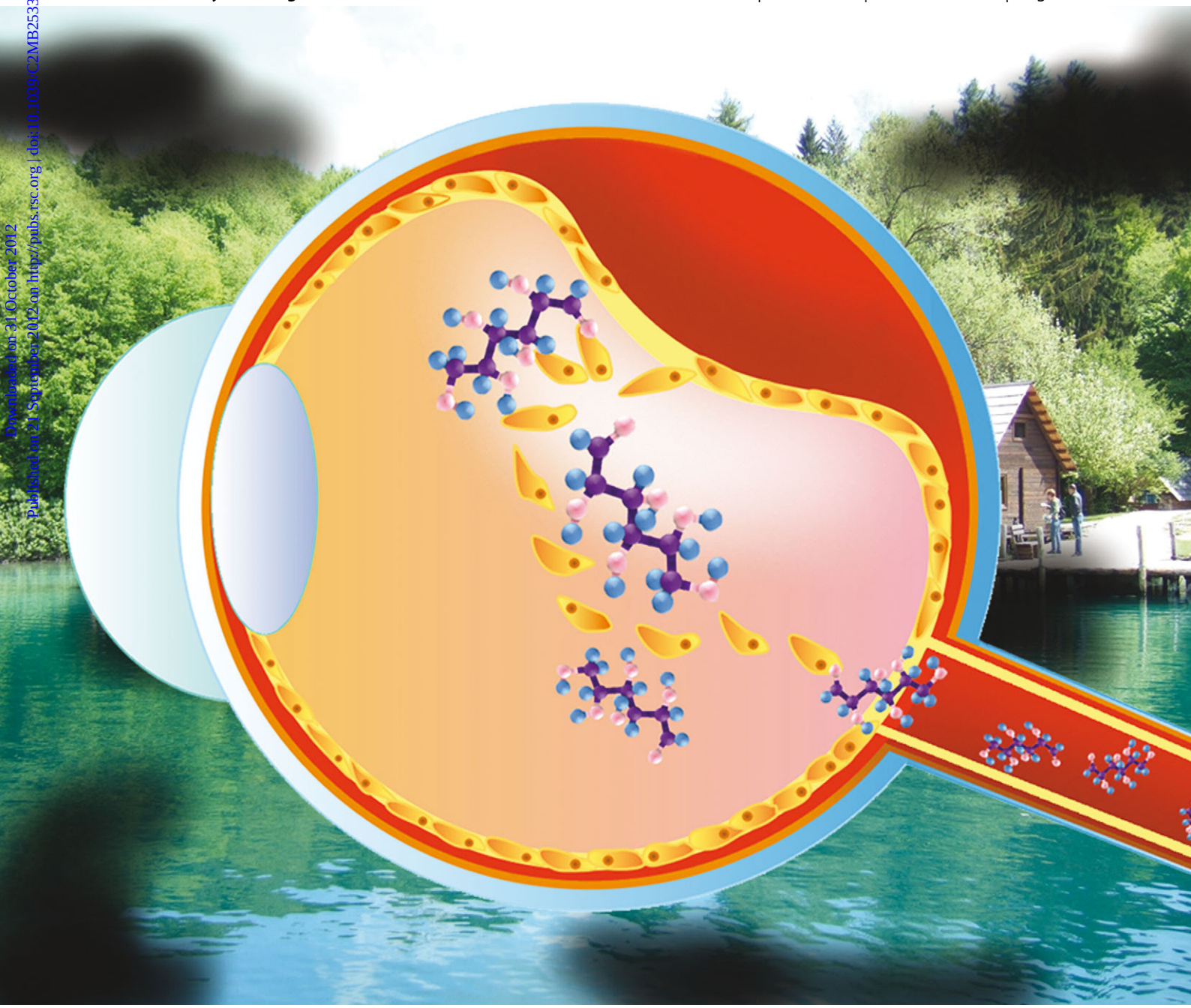

ISSN 1742-206X

RSC Publishing

PAPER

Hong-Lin Chan *et al.*

High glucose-induced proteome alterations in retinal pigmented epithelium cells and its possible relevance to diabetic retinopathy

1742-206X(2012)8:12;1-W

Molecular BioSystems

Dynamic Article Links
View Online

Cite this: *Mol. BioSyst.*, 2012, **8**, 3107–3124

www.rsc.org/molecularbiosystems

PAPER

High glucose-induced proteome alterations in retinal pigmented epithelium cells and its possible relevance to diabetic retinopathy†

You-Hsuan Chen, Jing-Yi Chen, Yi-Wen Chen, Szu-Ting Lin and Hong-Lin Chan*

Received 13th August 2012, Accepted 20th September 2012
DOI: 10.1039/c2mb25331c

Diabetic retinopathy can cause poor vision and blindness. Previous research has shown that high blood glucose weakens retinal capillaries and induces glycoxidation. However, the detailed molecular mechanisms underlying the effects of high blood glucose on development of diabetic retinopathy have yet to be elucidated. In this study, we cultured a retinal pigmented epithelium cell line (ARPE-19) in mannitol-balanced 5.5 mM, 25 mM, and 100 mM D-glucose media, and evaluated protein expression and redox-regulation. We identified 56 proteins that showed significant changes in protein expression, and 33 proteins showing significant changes in thiol reactivity, in response to high glucose concentration. Several proteins that are involved in signal transduction, gene regulation, and transport showed significant changes in expression, whereas proteins involved in metabolism, transport, and cell survival displayed changes in thiol reactivity. Further analyses of clinical plasma specimens confirmed that the proteins lamin B2, PUMA, WTAP, ASGR1, and prohibitin 2 showed type 2 diabetic retinopathy-dependent alterations. In summary, in this study, we used a comprehensive retinal cell-based proteomic approach for the identification of changes in protein expression and redox-associated retinal markers induced by high glucose concentration. Some of the identified proteins have been validated with clinical samples and provide potential targets for the prognosis and diagnosis of diabetic retinopathy.

1. Introduction

The retina is a light-sensitive nerve layer that can construct images of objects at the back of the eye. This specialized tissue is supplied with oxygen and nutrients from adjacent tiny blood vessels. Retinopathy is a retinal disease that occurs in approximately 25% of diabetic patients.[1,2] Diabetic retinopathy can cause poor vision and blindness because high blood glucose weakens retinal capillaries, leading to the leakage of blood into surrounding spaces. This bleeding can also cause scar formation, potentially leading to retinal detachment and disconnection from the wall of the eye. The detailed underlying molecular mechanisms and diagnostic biomarkers of diabetic retinopathy have yet to be fully elucidated.[3–7]

Hyperglycemia is a common feature of diabetes mellitus and is characterized by the modification of amino groups on proteins with monosaccharides. This reaction modifies the structure and function of proteins through the formation of advanced glycation end products and the generation of reactive oxygen species (ROS) in a process called glycoxidation.[8] The glycated proteins interact with membrane receptors, resulting in induction of intracellular oxidative stress, activation of a panel of protein kinases, and proinflammatory status.[9–12] Excess glucose-induced oxidative stress also promotes the development of diabetic complications, leading to tissue damage.[13]

Several chemical groups have been found to be potential targets of ROS in cells. One of these, the free thiol group (RSH) of cysteine residues is a potent nucleophilic agent and is able to undergo a number of redox-induced modifications under physiological conditions. Oxidative modifications of RSH groups other than disulphide formation include the formation of the sulfenic acid, sulfinic acid and sulfonic acid, depending upon the oxidative capacity of the oxidant.[14] Oxidation of RSH groups to sulfinic and sulfonic acids is an irreversible reaction under physiologic conditions and induces loss of biological functions of proteins.[15,16]

Two-dimensional gel electrophoresis (2-DE) is one of the most widely used proteomic separation techniques which has often been employed for the analysis of differentially expressed proteins in biological samples.[17,18] However, 2-DE and the methods commonly used for in-gel protein visualization are inherently variable and many replicate gels must be run before significant differences in protein expression can be ascribed accurately. Moreover, these protein visualization strategies often have narrow linear dynamic ranges of detection, making them

Institute of Bioinformatics and Structural Biology & Department of Medical Sciences, National Tsing Hua University, No.101, Kuang-Fu Rd. Sec.2, Hsinchu, 30013, Taiwan. E-mail: hlchan@life.nthu.edu.tw; Fax: +886-3-5715934; Tel: +886-3-5742476

† Electronic supplementary information (ESI) available. See DOI: 10.1039/c2mb25331c

unsuitable for the analysis of biological samples where protein copy numbers vary enormously. A significant improvement in the ability to use gel-based methods for protein quantification and detection was achieved with the introduction of 2D-difference gel electrophoresis (2D-DIGE), which can aid in co-detection of several biological samples on the same 2-DE gel, so reducing gel-to-gel variation.[19–23]

This study evaluated changes in retinal protein expression associated with high glucose concentration using lysine- and cysteine-labeling 2D-DIGE.[24,25] Combined strategies of MALDI-TOF MS and clinical specimen analysis further confirmed the changes in protein expression and redox-associated retinal markers induced by high glucose concentrations. Our results indicated potential targets for the prognosis and diagnosis of diabetic retinopathy. To our knowledge, this is the first study to report the effects of high glucose concentration on protein expression and redox regulation in retinal pigmented epithelium cells and to associate these findings with diabetic retinopathy.

2. Materials and methods

2.1 Chemicals and reagents

Generic chemicals were purchased from Sigma-Aldrich (St. Louis, USA), while reagents for lysine-2D-DIGE were purchased from GE Healthcare (Uppsala, Sweden). The synthesis of the ICy3 and ICy5 dyes has been previously reported.[26,27] All primary antibodies were purchased from GeneTex (Hsinchu, Taiwan) and anti-mouse, and anti-rabbit secondary antibodies were purchased from GE Healthcare (Uppsala, Sweden). All the chemicals and biochemicals used in this study were of analytical grade.

2.2 Cell lines and cell cultures

The ARPE-19 cell lines were purchased from the American Type Culture Collection (Manassas, VA) and maintained in Dulbecco's Modified Eagle's medium (DMEM) supplemented with 10% (v/v) fetal calf serum (FCS), L-glutamine (2 mM), streptomycin (100 μg mL^{-1}), and penicillin (100 IU mL^{-1}) (all from Gibco-Invitrogen Corp., UK). ARPE-19 cells were incubated at 37 °C in 5% CO_2.

For cell culturing at differential glucose concentrations, the cultures were exposed to D-glucose at a final concentration of 25 and 100 mM (corresponding to 2 h after meal plasma glucose levels of diabetic patients and glucose levels in uncontrolled diabetic patients,[28] respectively) and compared with cultures exposed to 5.5 mM D-glucose as control (corresponding to fasting plasma glucose levels of diabetes-free people).[29,30] To exclude the possible effects of hyperosmotic stress, mannitol was used to balance the differential glucose concentrations according to a previous report.[31] After exposure for at least 3 weeks, the monolayer cultures were used for further analysis.

2.3 MTT cell viability assay

ARPE-19 cells maintained in mannitol-balanced 5.5 mM, 25 mM and 100 mM glucose, respectively, for at least 3 weeks were trypsinized, counted using a haemocytometer and 5000 cells per well were seeded into 96-well plates. The culture was then incubated in mannitol-balanced 5.5 mM, 25 mM and 100 mM glucose for 24 h followed by removal of the medium. 50 μL of MTT working solution (1 mg mL^{-1}) (Sigma) was added to the cells in each well, followed by a further incubation at 37 °C for 4 h. The supernatant was carefully removed; 100 μL of DMSO was added to each well and the plates were shaken for 20 min. The absorbance of samples was then measured at a wavelength of 540 nm in a multi-well plate reader. Values were normalized against the untreated samples and were averaged from 8 independent measurements.

2.4 Flow cytometry analysis for apoptosis detection

An annexin-V/propidium iodide (PI) double assay was performed using the Annexin V, Alexa Fluor® 488 Conjugate Detection kit (Life technologies). Following ARPE-19 growth in differential glucose concentration media, cells were trypsinized from culture dish and washed twice with cold PBS. ARPE-19 cells (10^6) were resuspended in 500 μL binding buffer and stained with 5 μL Alexa Fluor 488 conjugated annexin V according to the manufacturer's instructions. 1 μL 100 μg mL^{-1} propidium iodide (PI) was added and mixed gently to incubate with cells for 15 min at room temperature in the dark. After the incubation period, samples were subjected to FCM analysis for 1 h using BD Accuri C6 Flow Cytometry (BD Biosciences, San Jose, CA). The data were analyzed using Accuri CFlow@ and CFlow Plus analysis software (BD Biosciences).

2.5 Assay for endogenous reactive oxygen species using DCFH-DA

ARPE-19 cells maintained in mannitol-balanced 5.5 mM, 25 mM and 100 mM glucose, respectively, for at least 3 weeks were trypsinized, counted using a haemocytometer and 10 000 cells per well were seeded into multiple 24-well plates. The culture was then incubated in mannitol-balanced 5.5 mM, 25 mM and 100 mM glucose for 24 h. After two washes with PBS, cells were treated with 10 μM of 2,7-dichlorofluorescin diacetate (DCFH-DA; Molecular Probes) at 37 °C for 20 min, and subsequently washed with PBS. Fluorescence was recorded at an excitation wavelength of 485 nm and emission wavelength of 530 nm.

2.6 Sample preparation for total cellular protein and thiol reactivity analysis

For total cellular protein analysis, cells were washed in chilled 0.5 × PBS and scraped in 2-DE lysis buffer containing 4% w/v CHAPS, 7 M urea, 2 M thiourea, 10 mM Tris–HCl, pH 8.3, 1 mM EDTA. Lysates were homogenized by passage through a 25-gauge needle 10 times, insoluble material was removed by centrifugation at 14 100 g for 30 min at 4 °C, and protein concentrations were determined using Coomassie Protein Assay Reagent (BioRad). Protein samples were labeled with *N*-hydroxy succinimidyl ester-derivatives of the cyanine dyes Cy2, Cy3 and Cy5. Briefly, 150 μg of protein sample was minimally labeled with 375 pmol of either Cy3 or Cy5 for comparison on the same 2-DE. To facilitate image matching and cross-gel statistical comparison, a pool of all samples was

also prepared and labeled with Cy2 at a molar ratio of 2.5 pmol Cy2 per μg of protein as an internal standard for all gels. Thus, the triplicate samples and the internal standard could be run and quantified by multiple 2-DE. The labeling reactions were performed in the dark on ice for 30 min and then quenched with a 20-fold molar ratio excess of free L-lysine to dye for 10 min. The differentially Cy3- and Cy5-labeled samples were then mixed with the Cy2-labeled internal standard and reduced with dithiothreitol for 10 min. IPG buffer, pH 3–10 nonlinear (2% (v/v), GE Healthcare) was added and the final volume was adjusted to 450 μL with 2D-lysis buffer for rehydration. All samples were run in triplicate against the standard pool.

For redox DIGE analysis, cells were lysed in 2-DE buffer (4% w/v CHAPS, 8 M urea, 10 mM Tris–HCl pH 8.3 and 1 mM EDTA) in the presence of ICy3 or ICy5 (80 pmol mg^{-1} protein) on ice to limit post-lysis thiol modification. Test samples were labeled with the ICy5 dye and mixed with an equal amount of a standard pool of both samples labeled with ICy3. Since ICy dyes interfered with the protein assay, protein concentrations were determined on replica lysates not containing dye. Lysates were left in the dark for 1 h followed by labeling with Cy2 to monitor the protein level. The reactions were quenched with DTT (65 mM final concentration) for 10 min followed by L-lysine (20-fold molar ratio excess of free L-lysine to Cy2 dye) for a further 10 min. Volumes were adjusted to 450 μL with buffer plus DTT and IPG buffer for rehydration. All samples were run in triplicate against the standard pool.

The rehydration process was performed with immobilized non-linear pH gradient (IPG) strips (pH 3–10, 24 cm) which were later rehydrated by CyDye-labeled samples in the dark at room temperature overnight (at least 12 hours). Isoelectric focusing was then performed using a Multiphor II apparatus (GE Healthcare) for a total of 62.5 kV h at 20 °C. Strips were equilibrated in 6 M urea, 30% (v/v) glycerol, 1% SDS (w/v), 100 mM Tris–HCl (pH8.8), 65 mM dithiothreitol for 15 min and then in the same buffer containing 240 mM iodoacetamide for another 15 min. The equilibrated IPG strips were transferred onto 26 × 20 cm 12.5% polyacrylamide gels casted between low fluorescent glass plates. The strips were overlaid with 0.5% (w/v) low melting point agarose in a running buffer containing bromophenol blue. The gels were run in an Ettan Twelve gel tank (GE Healthcare) at 4 Watt per gel at 10 °C until the dye front had completely run off the bottom of the gels. Afterward, the fluorescence 2-DE were scanned directly between the low fluorescent glass plates using an Ettan DIGE Imager (GE Healthcare). This imager is a charge-coupled device-based instrument that enables scanning at different wavelengths for Cy2-, Cy3-, and Cy5-labeled samples. Gel analysis was performed using DeCyder 2-D Differential Analysis Software v7.0 (GE Healthcare) to co-detect, normalize and quantify the protein features in the images. Features detected from non-protein sources (*e.g.* dust particles and dirty backgrounds) were filtered out. Spots displaying a γ 1.5 average-fold increase or decrease in abundance or spots displaying a γ 1.3 average-fold increase or decrease in thiol reactivity with a p-value <0.05 were selected for protein identification.

2.7 Protein staining

Colloidal coomassie blue G-250 staining was used to visualize CyDye-labeled protein features in 2-DE. Bonded gels were fixed in 30% v/v ethanol, 2% v/v phosphoric acid overnight, washed three times (30 min each) with ddH_2O and then incubated in 34% v/v methanol, 17% w/v ammonium sulphate, 3% v/v phosphoric acid for 1 h, prior to adding 0.5 g per liter coomassie blue G-250. The gels were then left to stain for 5–7 days. No destaining step was required. The stained gels were then imaged on an ImageScanner III densitometer (GE Healthcare), which processed the gel images as .tif files.

2.8 In-gel digestion

Excised post-stained gel pieces were washed three times in 50% acetonitrile, dried in a SpeedVac for 20 min, reduced with 10 mM dithiothreitol in 5 mM bicarbonate pH 8.0 for 45 min at 50 °C and then alkylated with 50 mM iodoacetamide in 5 mM ammonium bicarbonate for 1 h at room temperature in the dark. The gel pieces were then washed three times in 50% acetonitrile and vacuum-dried before reswelling with 50 ng of modified trypsin (Promega) in 5 mM ammonium bicarbonate. The pieces were then overlaid with 10 μL of 5 mM ammonium bicarbonate and trypsinized for 16 h at 37 °C. Supernatants were collected, peptides were further extracted twice with 5% trifluoroacetic acid in 50% acetonitrile and the supernatants were pooled. Peptide extracts were vacuum-dried, resuspended in 5 μL ddH_2O, and stored at −20 °C prior to MS analysis.

2.9 Protein identification by MALDI-TOF MS

For protein identification, extracted peptides were subjected to peptide mass fingerprinting (PMF) using MALDI-TOF MS. Briefly, 0.5 μL of a trypsin digested protein sample was mixed with 0.5 μL of a matrix solution containing α-cyano-4-hydroxy-cinammic acid at a concentration of 1 mg mL^{-1} of 50% ACN/0.1% TFA (v/v), spotted onto an anchorchip target plate (Bruker Daltonics) and dried. The peptide mass fingerprints were acquired using an Autoflex III mass spectrometer (Bruker Daltonics) in reflector mode and the raw data were analyzed with FlexAnalysis acquisition software (version 3.0, Bruker Daltonics). The algorithm used for spectral annotation was SNAP (Sophisticated Numerical Annotation Procedure). The following metrics were used: peak detection algorithm: SNAP; signal to noise threshold: 25; relative intensity threshold: 0%; minimum intensity threshold: 0; maximal number of peaks: 50; quality factor threshold: 1000; SNAP average composition: averaging; baseline subtraction: median; flatness: 0.8; median level: 0.5. The spectrometer was also calibrated with a peptide calibration standard (Bruker Daltonics) and internal calibration was performed using trypsin autolysis peaks at m/z 842.51 and m/z 2211.10 (MS BioTools version 3.0, Bruker Daltonics). Peaks in the mass range of m/z 800–3000 were used to generate a peptide mass fingerprint that was searched against the Swiss-Prot/TrEMBL database (2010_12, 515203 sequence entries) using Mascot software v2.3.00 (Matrix Science, London, UK). The following parameters were used: *Homo sapiens*; tryptic digest with a maximum of 1 missed cleavage; carbamidomethylation of cysteine, partial protein

N-terminal acetylation, partial methionine oxidation, partial modification of glutamine to pyroglutamate, ICy3 (C34 H44 N3 O) and ICy5 (C34 H42 N3 O) and a mass tolerance of 50 ppm. Identifications were accepted based on significant MASCOT scores ($P < 0.05$), spectral annotation and observed *versus* expected molecular weight and p*I* on 2-DE.

The classification of the biological functions and sub-cellular locations of these identified proteins are further determined based on a Swiss-Prot search (http://www.uniprot.org/) and KEGG pathway (http://www.genome.jp/kegg/) analysis.

2.10 Plasma sample collection and purification

Thirty donors in a single hospital (Chiayi Christian Hospital, Chiayi, Taiwan) were enrolled in the study. Those included in the study were divided into diabetic retinopathy patients ($n = 15$) and healthy donors ($n = 15$) with similar ages (50–60 years old). The criteria to assess the presence or absence of diabetic retinopathy were based on the pathological diagnosis and guidelines proposed by the World Health Organization. Diabetic retinopathy individuals were selected with significant retinopathy occurrence more than 5 years after diabetes diagnosed with ages between 50 and 60 years old. In contrast, healthy individuals were selected for healthy donors without diagnosed retinopathy and diabetes with ages between 50 and 60 years old. This study was approved by the Institutional Research Board and carried out according to the Helsinki Declaration Principles. Written informed consent was collected from all participating subjects.

2.11 Immunoblotting

Immunoblotting was used to validate the differential expression of mass spectrometry identified proteins. Cells were lysed with a lysis buffer containing 50 mM HEPES pH 7.4, 150 mM NaCl, 1% NP40, 1 mM EDTA, 2 mM sodium orthovanadate, 100 μg mL^{-1} AEBSF, 17 μg mL^{-1} aprotinin, 1 μg mL^{-1} leupeptin, 1 μg mL^{-1} pepstatin, 5 μM fenvalerate, 5 μM BpVphen and 1 μM okadaic acid prior to protein quantification with a Coomassie Protein Assay Reagent (BioRad). Protein samples (30 μg) were diluted in Laemmli sample buffer (final concentrations: 50 mM Tris pH 6.8, 10% (v/v) glycerol, 2% SDS (w/v), 0.01% (w/v) bromophenol blue) and separated by 1D-SDS-PAGE following standard procedures. After electroblotting separated proteins onto 0.45 μm Immobilon P membranes (Millipore), the membranes were blocked with 5% w/v skimmed milk in TBST (50 mM Tris pH 8.0, 150 mM NaCl and 0.1% Tween-20 (v/v)) for 1 h. Membranes were then incubated in primary antibody solution in TBS-T containing 0.02% (w/v) sodium azide for 2 h. Membranes were washed in TBS-T (3 × 10 min) and then probed with the appropriate horseradish peroxidase-coupled secondary antibody (GE Healthcare). After further washing in TBS-T, immunoprobed proteins were visualized using an enhanced chemiluminescence method (Visual Protein Co.).

2.12 Immunofluorescence

For immunofluorescence staining, cells were plated onto coverslips (VWR international) for overnight incubation. The cells were fixed with PBS containing 4% (v/v) *para*-formaldehyde for 25 min, washed three times with PBS, and followed by permeabilization in PBS containing 0.2% (v/v) Triton X-100 for 10 min. Coverslips were rinsed and blocked in PBS containing 5% (w/v) BSA for 10 min before incubation with primary antibodies diluted in 2.5% BSA/PBS for 1 h. After three washings with PBS, samples were incubated with the appropriate fluorescently labeled secondary antibodies diluted in 2.5% BSA/PBS for 1 h. Coverslips were then washed three times with PBS and at least twice with ddH_2O before mounting in Vectashield mounting medium (Vector Lab). Coverslip edges were sealed with nail polish onto glass slides (BDH) and then dried in the dark at 4 °C. For image analysis, cells were imaged using a Zeiss Axiovert 200 M fluorescent microscope (Carl Zeiss Inc., Germany). The laser intensities used to capture images were not saturated. Images were exported as .tif files using the Zeiss Axioversion 4.0 and processed using Adobe Photoshop V.7.0 software.

3. Results

3.1 High glucose concentration induces changes in protein expression in the retinal pigmented epithelium cell line ARPE-19

To evaluate the effects of high glucose concentration on the expression of retinal pigmented epithelium cell proteins, we cultured ARPE-19 cells in mannitol-balanced 5.5 mM, 25 mM,

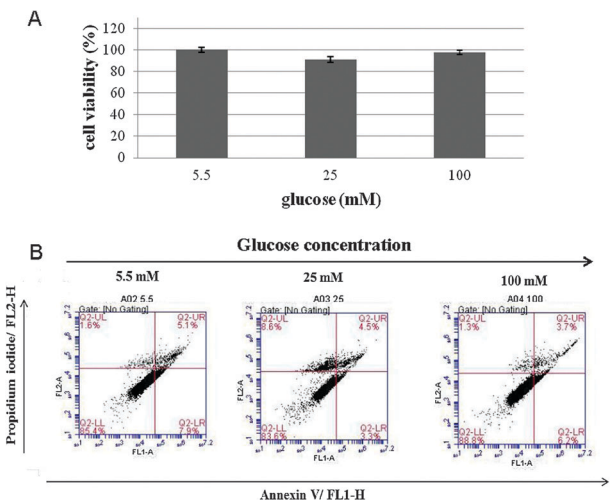

Fig. 1 Effect of glucose concentration on cell viability and cell apoptosis in ARPE-19. (A) MTT-based viability assays were performed on ARPE-19 cell cultures, following 3 weeks at different glucose concentrations (5.5 mM, 25 mM and 100 mM glucose). Paired Student *t*-test has been used for the statistical analysis of the experimental results. Values were normalized against untreated samples and are the average of 3 independent measurements ± the standard deviation. (B) 10^6 different glucose concentrations cultured ARPE-19 cells were incubated with Alexa Fluor 488 and propidium iodide in 1x binding buffer at room temperature for 15 min, and then stained cells were analyzed by flow cytometry to examine the effect of different glucose concentrations on apoptosis in APRE-19 cells. Annexin V is presented on the *x*-axis as FL1-H, and propidium iodide is presented on the *y*-axis as FL2-H. LR quadrant indicates the percentage of early apoptotic cells (Annexin V positive cells), and UR quadrant indicates the percentage of late apoptotic cells (Annexin V positive and propidium iodide positive cells).

Table 1 Alphabetic list of identified differentially expressed proteins after 2D-DIGE coupled with MALDI-TOF mass spectrometry analysis of ARPE-19 cells maintained in mannitol-balanced 5.5 mM, 25 mM and 100 mM glucose

No.	Swiss-prot No.	Protein name	p*I*	M_W	No. match. peptide	Cov. (%)	Score	25 mM/ 5.5 M[a]	*T*-test	100 mM/ 5.5 mM[a]	*T*-test	Subcellular location	Functional ontology	Match peptide sequences
1111	Q86TM9	Acetylcholinesterase	5.87	68 209	6/15	12	58/56	1.36	0.11	1.78	0.01	Secretion	Neuron transmission	R.AVLQSGAPNGPWATVGMGEA RR.R;K.TPGGPVSAFLGIPFAEPPM GPR.R
1229	Q86TM9	Acetylcholinesterase	5.87	68 209	7/14	14	74/56	2.99	0.01	2.38	0.0026	Secretion	Neuron transmission	R.EAPGNVGLLDQR.L; R.NYTAEEK.I
551	P27144	Adenylate kinase isoenzyme 4	8.41	25 336	4/9	21	71/56	1	0.97	−1.66	0.032	Mitochondrion	Metabolism	K.SLLVPDHVITR.L; R.GQHWLLD GFPR.T
874	P02511	Alpha-crystallin B chain	6.76	20 146	6/33	34	56/56	1.59	0.14	1.87	0.0095	Cytoplasm	Visual system	MDIAIHHPWIR.R;R.RPFFPFHSPS R.L
287	P08758	Annexin A5	4.94	35 971	4/11	11	57/56	1.3	0.24	1.7	0.044	Membrane	Coagulation	R.SEIDLFNIR.K;K.FITIFGTR.S
478	Q9Y6Q5	AP-1 complex subunit mu-2	8.22	48 192	4/6	14	58/56	1.42	0.00071	−1.22	0.0012	Cytoplasm	Transport	K.ILQEYITQQSNKLETGK.S;M.SA SAVFILDVK.G
78	P07306	Asialoglycoprotein receptor 1/ASGR1	5.28	33 735	5/13	16	64/56	−1.52	0.032	−1.29	0.09	Plasma membrane	Protein trafficking	R.WVCETELDK.A;K.QFVSDLR.S
607	Q9BXH1	Bcl-2-binding component 3/p53 up-regulated modulator of apoptosis/PUMA	9.09	20 691	5/16	27	65/56	1.27	0.17	1.77	0.014	Mitochondrion	Cell death	R.WPGGPRSRPR.G; R.QEGSSPEPVEGLAR.D
1118	Q9NZS5	Cell division protein kinase 11B	5.45	92 821	6/13	6	64/56	1.05	0.99	−1.56	0.022	Nucleus	Cell cycle	R.SPPRPPR.E; R.ISAEDGLK.H
870	O95813	Cerberus	7.7	30 577	4/9	18	69/56	1.56	0.081	1.59	0.013	Secretion	Signal transduction	R.QNQSSLSPVLLPR.N;K.VVVQN NLCFGK.C
1102	Q9NX63	Coiled-coil-helix-coiled-coil-helix domain-containing protein 3	8.48	26 421	4/5	17	59/56	1.27	0.076	1.51	0.028	Mitochondrion	Cytoskeleton	R.ERAAANEQLTR.A; K.ILQCYRENTHQTLK.C
374	Q14204	Cytoplasmic dynein 1 heavy chain 1	6.01	534 809	14/17	3	71/56	1.63	0.00071	1.46	0.01	Cytoplasm	Cytoskeleton	K.LFRSLAMTKPDR.Q;R.DLEASIA RYK.E
416	P15924	Desmoplakin	6.44	334 021	21/37	7	63/56	−1.66	0.0016	−1.57	0.0045	Cytoplasm	Cytoskeleton	R.MSQLEVK.E;K.RQVQNLVNK.S
986	P33981	Dual specificity protein kinase TTK	8.41	97 980	7/13	8	58/56	2.12	0.096	−1.3	0.65	Nucleus	Cell cycle	M.ESEDLSGR.E; K.QWQSKR.K
449	Q6UWE0	E3 ubiquitin-protein ligase LRSAM1	5.7	84 567	5/11	6	60/56	−1.87	0.0013	−1.67	0.0031	Cytoplasm	Protein degradation	R.MEQLMSITQEETESLR.R; R.VQELLDAAR.I
1136	Q6UWE0	E3 ubiquitin-protein ligase LRSAM1	5.7	84 567	6/23	8	57/56	−1.03	0.6	−2.97	0.0017	Cytoplasm	Protein degradation	R.MEQLMSITQEETESLR.R;R.VQE LLDAAR.I
137	Q96EB1	Elongator complex protein 4	8.75	47 014	5/10	8	59/56	1.69	0.12	2.51	0.041	Nucleus	Gene regulation	K.SNVTSFQR.R; K.YNIYSPLLFK.Y
30	Q96J88	Epithelial-stromal interaction protein 1	9.9	36 942	5/8	12	58/56	−1.57	0.0096	−1.45	0.0021	Cytoplasm	Cell migration	K.WKEQNR.A; R.EHQQYK.T
725	O75955	Flotillin-1	7.08	47 544	6/14	21	64/56	1.24	0.051	1.66	0.0091	Plasma membrane	Protein trafficking	R.GEAEAFAIGAR.A;K.AEAFQLY QEAAQLDMLLEK.L
335	Q14192	Four and a half LIM domains protein 2	7.8	34 166	6/17	19	71/56	1.55	0.02	1.61	0.055	Nucleus	Cell growth	K.GSSWHETCFICHR.C;R.QWHND CFNCK.K
761	Q16595	Frataxin	8.8	23 235	7/34	36	73/56	1.75	2.60×10^{-05}	−1.3	0.0051	Mitochondrion	Biosynthesis	R.AVAGLLASPSPAQAQTLTR.V;K. QSVYLMNLRK.S
1186	Q6ZVF9	G protein-regulated inducer of neurite outgrowth 3	7.52	83 357	5/7	5	57/56	1.42	0.11	−1.72	0.019	Plasma membrane	Neurite outgrowth	R.SQRTSNR.E;K.KQLGADSK.L
239	P04406	Glyceraldehyde-3-phosphate dehydrogenase	8.51	36 201	7/25	23	79/56	1.14	0.73	1.64	0.043	Cytoplasm	Glycolysis	K.VGVNGFGR.I;K.LTGMAFR.V

Table 1 (*continued*)

No.	Swiss-prot No.	Protein name	pI	M_W	No. match. peptide	Cov. (%)	Score	25 mM/ 5.5 M[a]	*T*-test	100 mM/ 5.5 mM[a]	*T*-test	Subcellular location	Functional ontology	Match peptide sequences
588	Q9UC36	Heat shock protein beta-1/HSP-27	5.98	22 826	5/24	24	69/56	1.27	0.013	1.83	0.0002	Cytoplasm	Protein folding	R.GPSWDPFR.D;K.LATQSNEITIP VTFESR.A
280	O00422	Histone deacetylase complex subunit SAP18	9.38	17 607	5/14	37	63/56	−1.56	0.0069	−1.53	0.0019	Nucleus	Gene regulation	K.EPEKPIDREK.T;R.KGTDDSMTL QSQK.F
613	P13645	Keratin, type I cytoskeletal 10	5.13	59 020	12/34	18	102/56	1.06	0.4	2.06	0.0012	Cytoplasm	Cytoskeleton	R.VLDELTLTK.A;K.SEITELRR.N
545	Q99612	Krueppel-like factor 6	6.46	32 529	4/5	12	67/56	−2.15	0.036	−4.16	0.0024	Nucleus	Gene regulation	K.IILAREK.K;R.CFSRSDHLALHM K.R
52	Q03252	Lamin-B2	5.29	67 762	11/34	16	58/56	−1.68	0.0017	−1.6	0.0024	Nucleus	Cytoskeleton	R.EELKEAR.M;K.LALDMEINAYR K.L
928	P19105	Myosin regulatory light chain 12A	4.67	19 839	4/19	29	56/56	1.3	0.17	1.74	0.0011	Cytoplasm	Cytoskeleton	R.NAFACFDEEATGTIQEDYLR.E; R.FTDEEVDELYR.E
1063	Q9Y2I1	Nischarin	5.04	168 292	8/14	7	62/56	1.5	0.013	1.72	0.0131.72	Endosome	Signal transduction	R.TFGPEREAEPAK.E ;MATARTFGPER.E
354	Q9UJ68	Peptide methionine sulfoxide reductase	8.22	26 410	4/9	15	57/56	1.29	0.12	1.53	0.0028	Cytoplasm	Redox regulation	K.EQTPVAAKHHVNGNR.T ;K.HHVNGNR.T
570	P30041	Peroxiredoxin-6	6	25 133	5/18	29	77/56	1.68	0.0056	1.6	0.0094	Cytoplasm	Redox regulation	M.PGGLLLGDVAPNFEANTTVGR. I;R.FHDFLGDSWGILFSHPR.D
55	Q9NUI1	Peroxisomal 2,4-dienoyl-CoA reductase	9.38	31 100	4/13	14	58/56	−1.53	0.0019	−1.42	0.044	Peroxisome	Fatty acid degradation	R.VNSLAPGPISGTEGLR.R;R.HLF CPDLLR.D
863	P30086	Phosphatidylethanolamine-binding protein 1	7.01	21 158	4/11	29	59/56	1.44	0.1	1.59	0.025	Cytoplasm	Cell signaling	K.NRPTSISWDGLDSGK.L;R.YVW LVYEQDRPLK.C
531	P18669	Phosphoglycerate mutase 1	6.67	28 900	5/27	31	72/56	1.55	0.0054	1.35	0.011	Cytoplasm	Metabolism	R.SYDVPPPPMEPDHPFYSNISK.D; R.FSGWYDADLSPAGHEEAK.R
1059	Q10471	Polypeptide *N*-acet-ylgalactosaminyltransfera se 2	8.63	65 433	7/13	11	58/56	−1.6	0.014	−1.56	0.028	Golgi apparatus	Biosynthesis	R.FLEQQNQVLQTK.W;R.SGGGFS SGSAGIINYQR.R
594	Q15007	Pre-mRNA-splicing regulator WTAP	5.12	44 388	7/16	15	70/56	1.06	0.4	2.06	0.0012	Nucleus	Gene regulation	R.TSGSGFHR.E;R.ENILVMRLATK .E
764	Q5GLZ8	Probable E3 ubiquitin-protein ligase HERC4	5.8	119 913	5/11	5	57/56	−1.94	0.00017	−1.69	0.0118	Cytoplasm	Protein degradation	R.YVPNLLK.S;K.ELVLNGADTAV NK.Q
1183	P07737	Profilin-1	8.44	15 126	3/8	26	57/56	1.6	0.0076	1.25	0.081	Cytoplasm	Cytoskeleton	R.DSLLQDGEFSMDLR.T;K.STGG APTFNVTVTK.T
73	Q8WXW	Progesterone-induced-block-ing factor 1	5.77	90 035	7/12	9	58/56	−1.53	0.037	−1.22	0.026	Cytoplasm	Cell signaling	K.TNQEIDQLRNASR.E;K.QLTETY EEDR.K
1200	Q99623	Prohibitin-2	9.83	33 276	ell	16	57/56	−1.33	0.13	−1.71	0.028	Mitochondrion	Cell growth	M.AQNLKDLAGR.L ;R.IYLTADNLVLNLQDESFTR.G
114	Q8WUD1	Ras-related protein Rab-2B	7.68	24 227	4/7	25	63/56	−1.62	0.006	−1.81	0.0022	Plasma membrane	Protein trafficking	.MTYAYLFKYIIIGDTGVGK.S;R.Q HSSSNMVIMLIGNK.S
1067	P62070	Ras-related protein R-Ra2	5.74	23 613	5/14	24	58/56	1.41	0.071	1.51	0.0025	Plasma membrane	Signal transduction	R.QVTQEEGQQLARQLK.V; K.ADLDHQR.Q
236	P48443	Retinoic acid receptor RXR-gamma	7.55	51 580	5/10	8	60/56	1.14	0.73	1.64	0.043	Nucleus	Gene regulation	K.SELGCLR.A;K.CLEHLFFFK.L
490	P48443	Retinoic acid receptor RXR-gamma	7.55	51 580	4/8	7	57/56	−1.18	0.3	−1.78	0.011	Nucleus	Gene regulation	K.SELGCLR.A;K.YPEQPGR.F
572	P48443	Retinoic acid receptor RXR-gamma	7.55	51 580	6/17	8	57/56	−1.97	0.0025	−1.7	0.0027	Nucleus	Gene regulation	K.CLVMGMK.R;.MYGNYSHFMK. F
658	P48443	Retinoic acid receptor RXR-gamma	7.55	51 580	5/13	8	63/56	−1.75	0.0057	−1.53	0.021	Nucleus	Gene regulation	K.CLVMGMK.R; K.YPEQPGR.F
1145	P48443	Retinoic acid receptor RXR-gamma	7.55	51 580	5/15	8	60/56	−1.35	0.1	−1.56	0.028	Nucleus	Gene regulation	K.SELGCLR.A; K.CLVMGMK.R

Table 1 *(continued)*

No.	Swiss-prot No.	Protein name	pI	M_w	No. match. peptide	Cov. (%)	Score	25 mM/5.5 M[a]	*T*-test	100 mM/5.5 mM[a]	*T*-test	Subcellular location	Functional ontology	Match peptide sequences
347	Q9Y5M8	Signal recognition particle receptor subunit beta	9.17	29 912	4/6	17	62/56	−1.5	0.027	−1.66	6.20×10^{-05}	ER	Protein synthesis	IK.QDIAMAKSAK.L;K.VEFLECSA K.G
268	Q9BX26	Synaptonemal complex protein 2	9.01	177 239	9/12	7	67/56	1.31	0.094	1.52	0.019	Nucleus	Cell cycle	K.VYAHQMVR.T;K.LYLLNTTK.L
83	Q9BV79	Trans-2-enoyl-CoA reductase	8.99	40 744	6/11	13	78/56	−1.26	0.03	−1.51	0.0041	Mitochondrion	Fatty acid synthesis	K.SLGAEHVITEEELR.R;R.GFWLS QWKK.D
495	Q13595	Transformer-2 protein homolog alpha	11.27	32 726	6/19	23	59/56	−1.65	0.01	−1.97	0.0059	Nucleus	Gene regulation	R.AHTPTPGIYMGRPTHSGGGGG GGGGGGGGGGGR.R; R.SGSRSPSR.V
606	Q9NVH6	Trimethyllysine dioxygenase	7.64	50 113	8/28	15	61/56	1.84	0.0081	1.95	0.0007	Mitochondrion	Biosynthesis	R.WYTAHR.T;R.RPENEFWVKLKP GR.V
296	Q96IK2	Tropomyosin alpha-1 chain	4.69	32 746	12/44	28	88/56	1.73	0.18	2.01	0.023	Cytoplasm	Cytoskeleton	K.MEIQEIQLKEAK.H;R.KLVIIESD LER.A
719	Q9H0Y0	Ubiquitin-like-conjugating enzyme ATG10	5.35	25 718	3/4	13	62/56	−1.68	0.0024	−1.44	0.019	Cytoplasm	Protein degradation	K.TNEFMTPVLK.N;K.DCSDGYMC K.I
573	P11172	Uridine 5′-monophosphate synthase	6.81	52 645	5/10	8	57/56	1.44	0.051	1.68	0.01	Cytoplasm	Biosynthesis	K.RGSDIIIVGR.G;K.SGLSSPIYIDL R.G

[a] Average ratio of differential expression ($p < 0.05$) between ARPE-19 maintained in 5.5 mM, 25 mM and 100 mM glucose concentrations calculated from triplicate gels.

and 100 mM glucose media for at least 3 weeks. We then performed MTT and apoptotic assays. Results indicated that the ARPE-19 cells showed nonsignificant differences in viability and apoptosis among the 3 culture conditions (Fig. 1A and B). We then evaluated protein expression in the ARPE-19 cells, and identified 1369 protein spots and 111 protein features that displayed differential expression among the 3 conditions (≥1.5-fold changes; $p < 0.05$). We used MALDI-TOF MS to identify proteins in 56 of these features (Table 1, Fig. 2 and 3). The differentially expressed proteins were predominantly located in the cytoplasm, nuclei, and mitochondria, and function in signal transduction, gene regulation, and transport (Fig. 4 and Table 1).

To further verify the upregulation or downregulation of the identified proteins, we performed immunoblot analysis of proteins modulated by high glucose concentrations (25 mM and 100 mM) and compared them with proteins in control cells (5.5 mM glucose) (Fig. 5). We used specific antibodies against peroxinredoxin 6, GAPDH, lamin-B2, tropomyosin 1, prohibitin 2, and HSP-27. As shown in Fig. 5, 2D-DIGE analysis provided further evidence of changes in protein expression in response to glucose treatment (Table 1).

3.2 Clinical validation of findings using diabetic retinopathy plasma specimens

We analyzed diabetic retinopathy plasma specimens using immunoblotting and ELISA to confirm the clinical relevance of proteomic analysis findings. Results indicated that levels of 20 kDa p53 upregulated modulator of apoptosis (PUMA) and 44 kDa pre-mRNA-splicing regulator (WTAP) levels were increased significantly in the plasma of diabetic retinopathy patients compared to plasma from healthy donors. These proteins might, therefore, provide potential candidates for the diagnosis of diabetic retinopathy. Levels of 68 kDa lamin B2, 34 kDa asialoglycoprotein receptor 1 (ASGR1), and 33 kDa prohibitin 2 were decreased significantly in the plasma of patients with diabetic retinopathy, compared to plasma from healthy controls. These findings were consistent with data from 2D-DIGE and MALDI-TOF MS, and further suggested that the identified proteins could potentially be used as indicators of diabetic retinopathy (Fig. 6 and ESI†).

3.3 Redox proteomic analysis of high glucose-induced cysteine modifications in ARPE-19 proteins

High glucose concentrations reportedly induce ROS, which weaken the retinal capillaries and cause leakage of blood into the surrounding space. Although cellular antioxidant reactions can balance low ROS concentrations, the accumulation of ROS induces modifications in biomolecules such as lipids, DNA, and proteins. The reduced thiol group of cysteine residues is a potent nucleophilic agent that undergoes a number of oxidative modifications leading to loss of protein function (see "Introduction"). To optimize conditions for the monitoring of oxidative stress-induced protein modifications, we used DCF fluorescence to detect high glucose-induced ROS production. Results showed that high glucose concentrations increased ROS production in ARPE-19 cells (Fig. 7). We then applied recently developed redox 2D-DIGE methodology

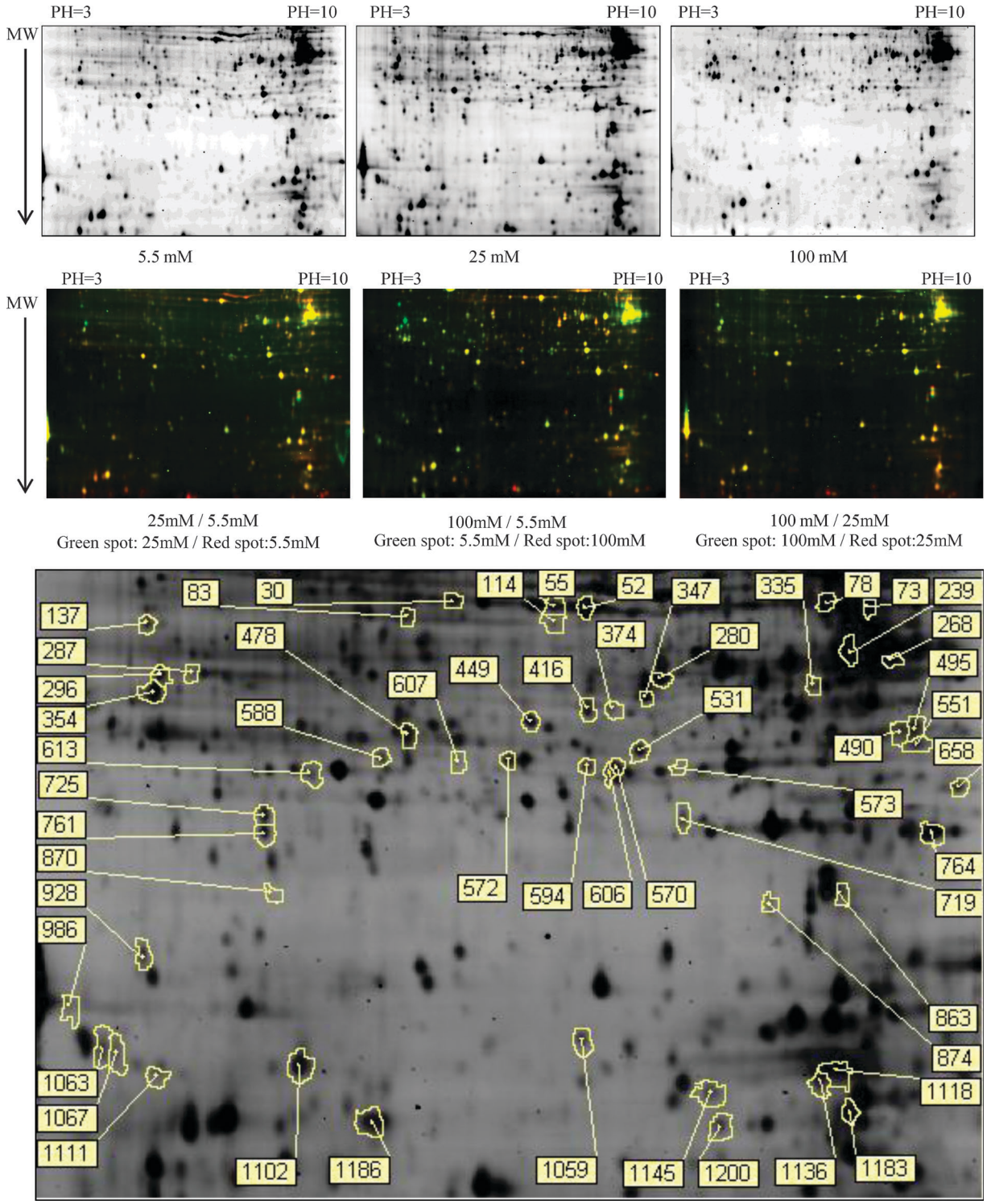

Fig. 2 2D-DIGE analysis of high glucose-dependent differentially expressed proteins in ARPE-19 cells. ARPE-19 cells maintained in 5.5 mM, 25 mM and 100 mM glucose were lysed and arranged for a triplicate 2D-DIGE experiment. Protein samples (150 μg each) were labeled with Cy-dyes and separated using 24 cm, pH 3–10 non-linear IPG strips. 2D-DIGE images of ARPE-19 incubated in 5.5 mM, 25 mM and 100 mM glucose at appropriate excitation and emission wavelengths were pseudo-colored and overlaid with ImageQuant Tool (GE Healthcare). The differentially expressed identified protein features are annotated with spot numbers.

using iodoacetylated cyanine (ICy) dyes to evaluate changes in protein thiol reactivity induced by high glucose levels. We compared ARPE-19 cells cultured in high glucose concentrations (25 mM and 100 mM) with ARPE-19 cells cultured in 5.5 mM glucose. These cells were lysed in the presence of ICy5 in triplicate. Individual ICy5-labeled samples were then run on 2-DE against an equal load of ICy3-labeled standard pool comprising an equal mixture of three sample types to aid

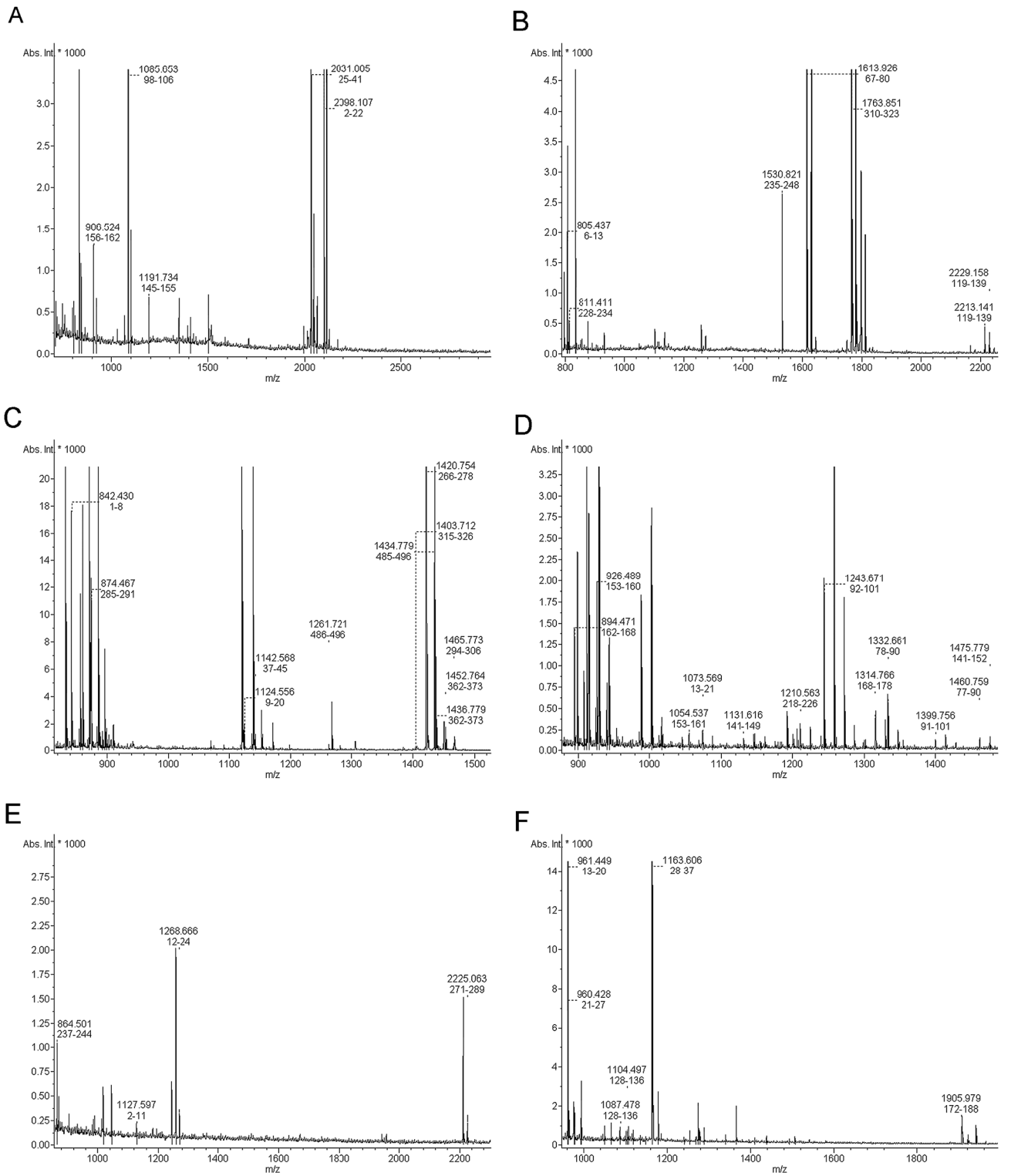

Fig. 3 Peptide mass fingerprinting of differentially expressed proteins ((A) peroxinredoxin 6 (B) GADPH (C) lamin-B2 (D) tropomyosin 1 (E) prohibitin 2 (F) HSP-27). Mass spectra were acquired on an Autoflex TOF/TOF mass spectrometer (Bruker Daltonics). Peptides contributing to protein identifications were marked with m/z values and sequence locations on proteins were searched against the Swiss-Prot/TrEMBL database (2010_12, 515203 sequence entries) using Mascot software v2.3.00 (Matrix Science, London, UK).

in spot matching and to improve the accuracy of quantification (Fig. 8). The ICy5-labeled samples were subsequently labeled with lysine labeling Cy2 dye as an internal protein level control which was used to normalize the corresponding ICy5/ICy3 signals (Table 2). We detected 2074 protein features, of which 408 displayed statistically significant changes in labeling, in response to high glucose concentrations. Comparison of our saturated cysteine-labeling 2D-DIGE images with the images

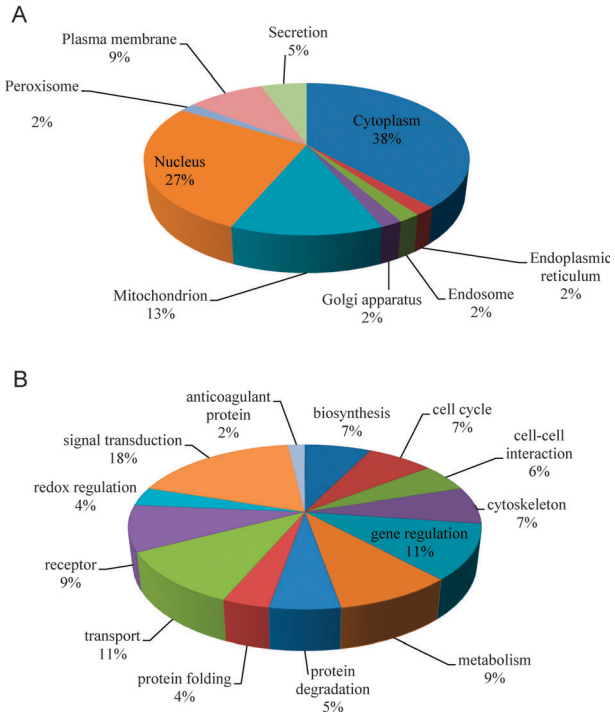

Fig. 4 Percentage of differentially expressed proteins identified by 2D-DIGE/MALDI-TOF MS for ARPE-19 cells incubated in 5.5 mM, 25 mM and 100 mM glucose according to their sub-cellular locations (A) and biological functions (B). The classification of the biological functions and sub-cellular locations of these identified proteins is done based on a Swiss-Prot search and KEGG pathway analysis.

obtained using the minimal lysine-labeling strategy revealed that precipitation increased significantly in proteins in the >75 kDa molecular weight range. The presence of ICy dye-modified cysteines in higher molecular weight proteins might have caused the observed increases in precipitation. We then performed poststaining with CCB, and matched stains with fluorescence images to select 152 gel features. We identified 33 of these features as unique gene products using MALDI-TOF peptide mass fingerprinting (Table 2). All of the identified proteins contained at least one cysteine (searched from Swiss-Prot database). Because the ICy dyes target reduced cysteinyl thiols, these results suggested that high glucose concentration modified the oxidative status of some of these thiol groups. We classified these identified proteins according to their subcellular locations and biological functions: 53% of the proteins were cytosolic, 13% were endoplasmic reticulum proteins, 13% were nuclear proteins, 9% were mitochondrial proteins, 6% were secreted proteins, and 6% were located in plasma membranes. The identified proteins were predominantly involved in metabolism (25%), transport (18%) and cell apoptosis (12%) (Fig. 9).

4. Discussion

In this study, we evaluated high glucose-induced changes in protein expression and thiol reactivity in retinal pigmented epithelium cells using lysine- and cysteine-labeling 2D-DIGE, respectively. Fifty-six proteins showed differential expression in ARPE-19 cells cultured in high glucose concentrations compared with control ARPE-19 cells. The majority of the proteins exhibited glucose concentration-dependent changes in expression in ARPE-19 cells cultured in 5.5 mM, 25 mM, and 100 mM glucose. However, almost 25% of the identified proteins, including frataxin, failed to display glucose concentration-dependent changes in expression in 100 mM glucose. This suggested that very high glucose concentrations might activate as yet unidentified mechanisms to reverse high glucose-induced changes in protein expression.

Previous *in vitro* studies have shown that high glucose concentrations induce the production of superoxide radicals through the autooxidation of glucose.[19,20] Studies have also reported an increase in protein oxidation products in the blood of diabetic patients. The most extensively investigated markers of protein oxidation are protein carbonyl groups leading to the formation of the oxidized side chains of lysine, proline, arginine, and threonine residues.[24–26] Cysteine is also highly susceptible to ROS-induced oxidation.[24] Our redox-proteomic results indicated that long-term incubation of cultured retinal pigmented epithelium cells to high glucose concentrations results in the oxidation of thiol groups on cysteine residues. This further evidenced that these cellular proteins are the intracellular targets of gluco-oxidation.

When analyzing changes in thiol reactivity in response to high glucose levels, we identified 33 proteins showing redox changes in the cysteine residues of specific proteins. These findings suggested that high glucose-induced oxidative stress disturbed the normal redox balance in ARPE-19 cells, leading to the redox modulation of specific proteins. The ICy labeling results supported the hypothesis that high glucose concentrations induces the formation of free thiols in certain proteins through the breakage of disulfide bonds, which increases ICy dye labeling. In addition, high glucose concentrations-induced ROS or protein-derived peroxides might then directly oxidize thiol groups to form the sulfenic, sulfinic, or sulfonic acid forms of cysteine, leading to decreased ICy dye labeling. These thiol modifications have been reported to disturb normal protein function.[32] Our results suggested that high glucose concentrations induce changes in protein expression and redox, which modify cell physiology and might contribute to the development of diabetic retinopathy.

In this study, we identified that proteins involved in redox regulation (peptide methionine sulfoxide reductase, peroxiredoxin-6, glutathione S-transferase Mu 5, and inducible NO synthase) and protein folding (heat shock protein β-1 (HSP27), heat shock 70 kDa protein 5, heat shock 70 kDa protein 9, and heat shock cognate 71 kDa protein) display increased expression or altered thiol reactivity in high glucose concentrations. Heat shock proteins are molecular chaperones that protect cells from harmful conditions by reducing the concentrations of denatured or unfolded proteins. The accumulation of damaged and misfolded proteins following exposure to toxic stimuli is a major cause of cell death.[33] Physiological and environmental stresses, including high glucose concentration-induced oxidative stress, upregulate the expression of heat shock protein 70 families and HSP27. Barutta *et al.*[34] reported that HSP27 is phosphorylated by the stress response protein p38 in hyperglycemic conditions. In addition,

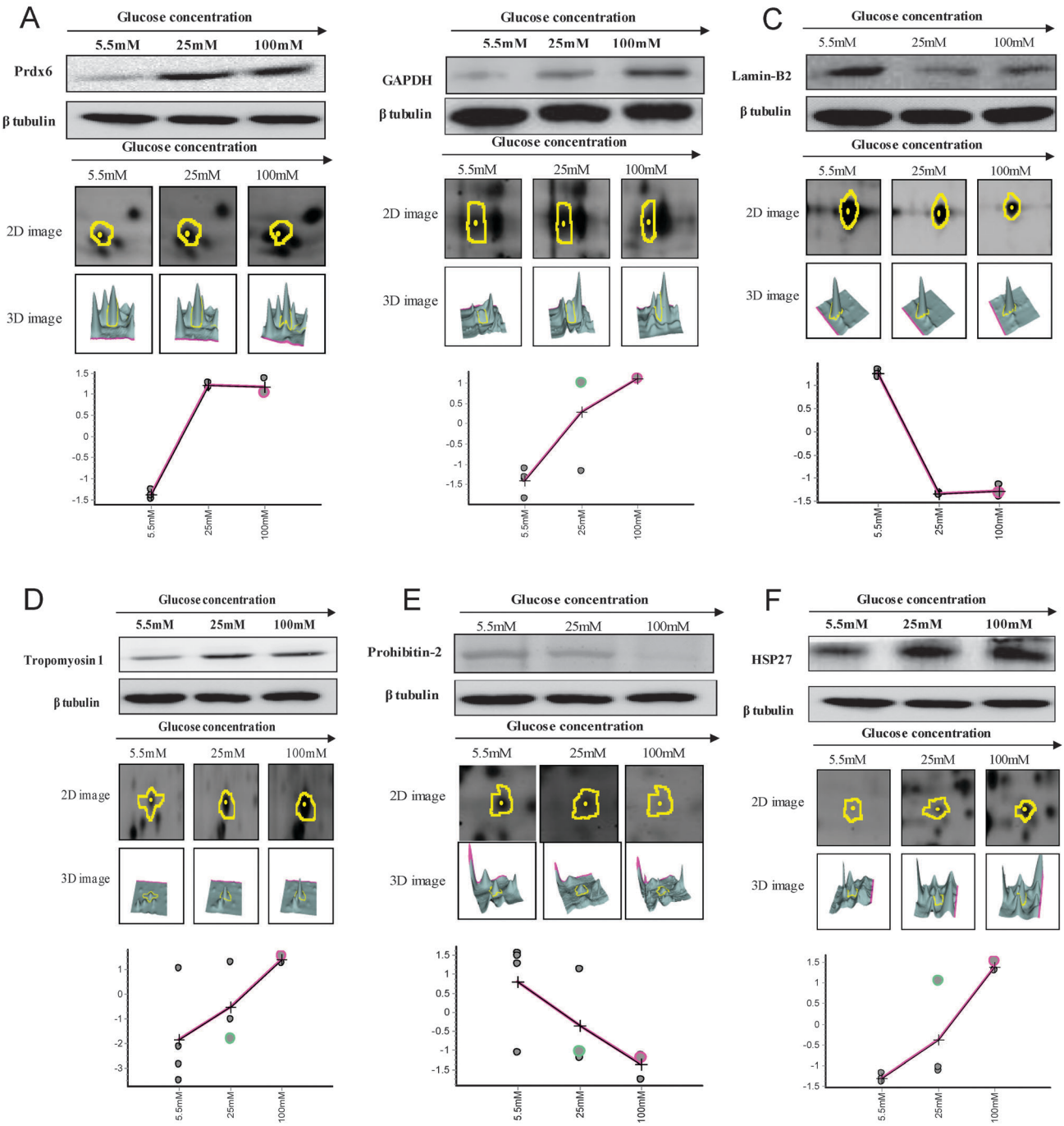

Fig. 5 Representative immunoblotting analyses and 2D-DIGE images for selected differentially expressed proteins ((A) peroxinredoxin 6 (B) GADPH (C) lamin-B2 (D) tropomyosin 1 (E) prohibitin 2 (F) HSP-27) identified by 2D-DIGE/MALDI-TOF MS for ARPE-19 cells incubated in 5.5 mM, 25 mM and 100 mM glucose. The levels of identified proteins, peroxinredoxin 6, GADPH, lamin-B2, tropomyosin 1, prohibitin 2 and HSP-27, in ARPE-19 cells maintained in 5.5 mM, 25 mM and 100 mM glucose were confirmed by immunoblot (top panels). β-Tubulin was used as loading control in this study. The levels of these intracellular proteins were also visualized by fluorescence 2-DE images (middle top panels), three-dimensional spot images (middle bottom panels) and protein abundance map (bottom panels).

heat shock protein 70 families are induced by cellular stresses and hyperglycemia in a diabetic nephropathy rat model. Our results indicated that high glucose concentrations upregulate the expression of heat shock and redox-regulating proteins in retinal pigmented epithelium cells, and influence their thiol reactivity. Further analyses using redox proteomic strategies confirmed the involvement of the identified proteins in protein folding and redox regulation in ARPE-19 cells. Glutathione S-transferase Mu 5, inducible NO synthase, and heat shock protein families all showed increased labeling in high glucose levels, suggesting that high glucose concentrations directly modulate the functions of these proteins by generating new free thiol groups.

Specific upregulation of heat shock proteins suggests the increased expression of unfolded proteins in the endoplasmic

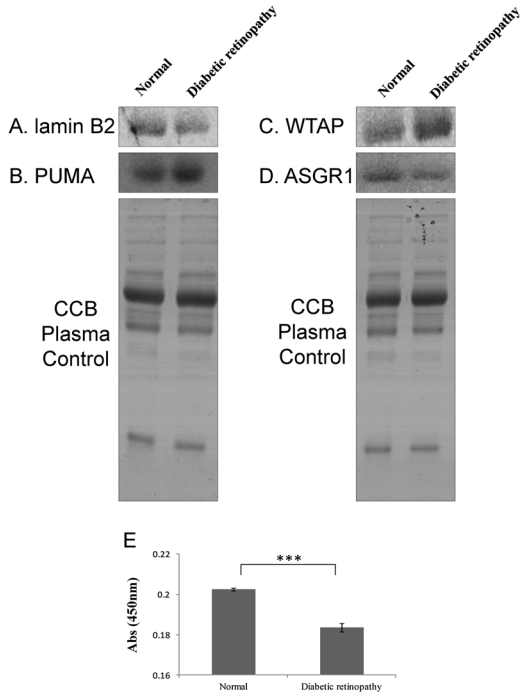

Fig. 6 Representative immunoblotting and ELISA analysis of lamin B2, PUMA, WTAP, ASGR1 and prohibitin 2 in plasma from type 2 diabetic patients with retinopathy and healthy donors. Plasma samples from 15 type 2 diabetic patients and 15 healthy donors were run in a pool. 20 μg of plasma samples were loaded and resolved by SDS-PAGE, followed by either immunoblotting with (A) lamin B2, (B) PUMA, (C) WTAP and (D) ASGR1 antibodies or staining with colloidal coomassie Blue G-250 as a loading control. (E) 50 μg of plasma samples were coated onto each well of a 96-well plate for ELISA analysis against prohibitin 2 and the absorbance was measured at 450 nm using a Stat Fax 2100 microtiterplate reader. Paired Student *t*-test has been used for the statistical analysis of the experimental results. *** Signifies a *p*-value of ≦0.001.

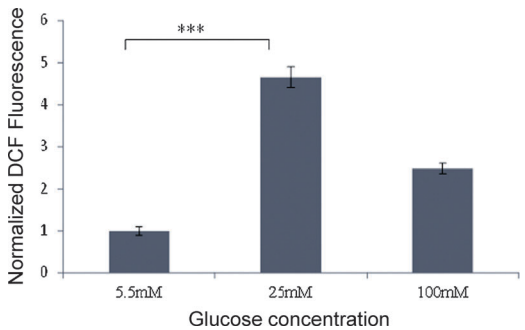

Fig. 7 Effect of high glucose on ARPE-19 ROS production. DCFH-based intracellular ROS production assays were performed where 10 000 ARPE-19 cells cultured in 5.5 mM, 25 mM and 100 mM glucose for at least 3 weeks were plated into 96-well plates in medium containing 10% FBS. After overnight incubation in 5.5 mM, 25 mM and 100 mM glucose, the cells were treated with 10 μM of DCFH-DA at 37 °C for 20 min and the fluorescence images was recorded at excitation and emission wavelengths of 485 nm and 530 nm, respectively. Paired Student *t*-test has been used for the statistical analysis of the experimental results. *** Signifies a *p*-value of ≦0.001.

reticulum (ER), which is associated with ER stress.[35] Several previous studies have identified ER stress in diabetes, observing increased levels of ER stress markers such as GRP94, CHOP, and BiP in a diabetic mouse model[36] and in pancreatic β cells of type 2 diabetic patients.[37] The ER plays a role in regulating intracellular calcium (Ca^{2+}) concentrations. Endoplasmic reticulum stress might contribute to Ca^{2+} release from the ER and stimulate mitochondrial disruption, which then influences cell survival.[38] In this study, we observed that high glucose concentrations disrupted heat shock 70 kDa protein 5 (GRP78), an ER chaperone protein responsible for maintaining the correct folding of ER proteins, causing ER stress. This mechanism might explain changes in the expression of Ca^{2+}-dependent proteins (such as annexin A5) in ARPE-19 cells treated with high glucose concentrations compared with control cells. Protein kinase C (PKC) is a member of the family of protein kinases that is involved in controlling the phosphorylation of downstream target proteins. Previous studies have reported that diacylglycerol and Ca^{2+} signaling activate PKC.[39,40] To investigate the hypothesis that increased Ca^{2+}, deriving from high glucose concentration-induced ER stress and phosphorylation of downstream targets, stimulates PKC, we performed immunostaining and immunoblotting analysis of phospho-PKC substrates. We identified that multiple PKC substrates increased phosphorylation in ARPE-19 cells cultured in 25 mM and 100 mM glucose compared with cells cultured in 5.5 mM glucose. Most of these phospho-PKC substrates were nuclear rather than cytosolic (Fig. 10).

In this study, we further observed the downregulation of proteins responsible for intracellular protein degradation, including E3 ubiquitin–protein ligase LRSAM1, E3 ubiquitin–protein ligase HERC4, and ubiquitin-like-conjugating enzyme ATG10. The ubiquitin pathway eliminates misfolded ER proteins in cells and plays an important role in physiological adaptation to ER stress. Defects in the ubiquitin system might, therefore, contribute to the accumulation of misfolded or unfolded ER proteins and cause ER stress.[41]

Our findings also indicated the downregulation of prohibitin (PHB) in ARPE-19 cells treated with high glucose concentrations. Prohibitin is a ubiquitously expressed protein that exhibits diverse functions at different cellular locations. It is predominantly located in the inner membrane of mitochondria, and functions as a chaperone protein that stabilizes mitochondrial DNA and maintains mitochondrial morphology.[42] In the study by Merkwirth *et al.*, PHB knockdown reduced the mitochondrial membrane potential significantly and abrogated complex I activity.[43] Schleicher *et al.* also suggested that the absence of PHB results in excess ROS formation, indicating that PHB might play an important role in the removal of ROS and maintenance of cell survival.[44] Prohibitin is also involved in transcriptional regulation, which is essential for cell proliferation and cell cycle regulation in the nucleus.[45] The PI3K/AKT pathway phosphorylates PHB on Thr258 and stimulates the MAPK pathway to promote cell proliferation. Phosphorylation of PHB on Thr258 contributes to the feedback that activates the PI3K/AKT pathway, leading to mitogenesis.[46] Our study suggested the down-regulation of PHB in retinal pigmented epithelium cells in response to high glucose concentrations, which rendered the cells unable to alleviate high glucose-induced mitochondrial oxidative stress, leading to the destabilization of mitochondria. Also, the study

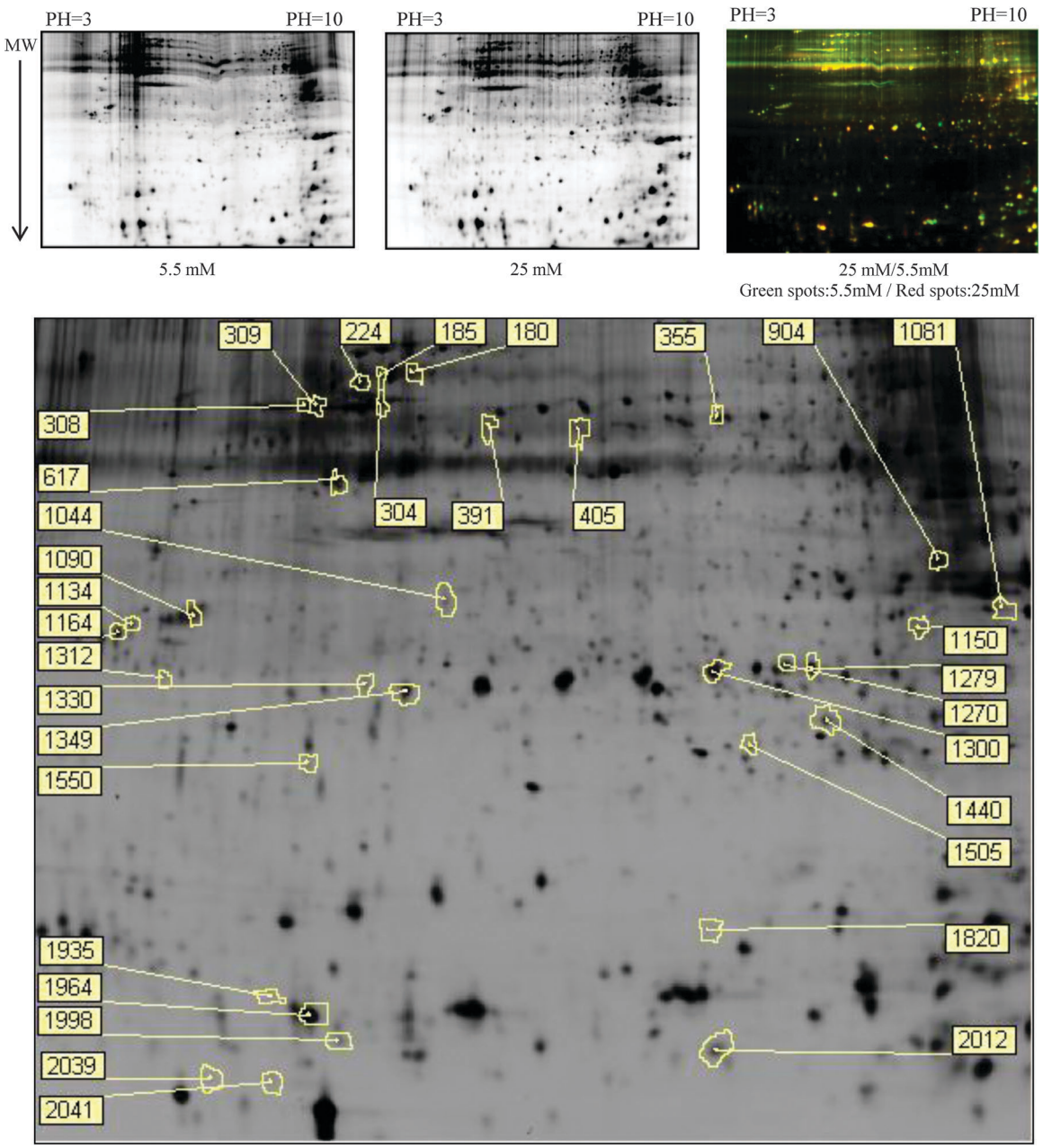

Fig. 8 Redox 2D-DIGE analysis of high glucose-induced differential cysteine-modification in ARPE-19 cells. Lysates from ARPE-19 cells cultured in 5.5 mM and 25 mM glucose for at least 3 weeks were subjected to redox 2D-DIGE analysis as described in Materials and Methods. 2-DE-proteome map of ARPE-19 cultured in mannitol-balanced 5.5 mM and 25 mM glucose are displayed. The differentially labeled protein features are annotated with spot numbers.

also proposed that down-regulation of PHB might disturb both MAPK and PI3K/AKT pathways, resulting in the reduction of cell proliferation.

Most cell junction proteins are plasma membrane-embedded transmembrane proteins; therefore, it is generally difficult to isolate them for biochemical analysis such as 2D-DIGE analysis. In this study, we identified that high glucose concentrations downregulated the transmembrane junction protein desmoplakin. This suggested that disruption of desmoplakin might play an important role in high glucose concentration-induced dysfunction of junctions in retinal pigmented epithelium cells. To our knowledge, our study is the first to associate desmoplakin with retinopathy. Inducible NO synthase (iNOS), which is expressed after cell activation and produces NO for physiological function, reportedly breaks down tight junctions in rat retinal pigmented epithelium cells through nitrosative/oxidative stress.[47,48] During our analyses, we identified the involvement of iNOS in redox modification at cysteine residues. High glucose concentrations might, therefore, activate iNOS and disrupt tight junctions to induce vessel leakage. Rho proteins play major roles in modulating cytoskeletal actin rearrangements in human retinal pigment epithelial cells.[49,50] The key regulator for Rho activity is Rho GTPase-activating protein, which is one of the cellular targets of the high glucose

Table 2 Differential cysteine labeled proteins identified by ICy 2D-DIGE and MALDI-TOF MS. Proteins displaying high glucose-induced differential labeling of cysteines using ICy dyes were identified by MALDI-TOF peptide mass mapping analysis. Proteins with thiol reactivity displaying an average fold-difference of ≥ 1.3-fold where $p < 0.05$ and spots matched in all images are shaded grey

No.	Swiss-prot No.	Protein name	p*I*	M_W	No. match. peptides	Cov. (%)	Score	25 mM/5.5 M (Cys/lys)[a]	Subcellular location	Functional ontology	Match peptide sequences
1550	P17516	Aldo-keto reductase family 1 member C4	6.46	37 442	7/10	12	66/56	1.8	Cytoplasm	Biotransformation	M.DPKYQR.V;MDPKYQR.V
405	Q9BPW4	Apolipoprotein L4	7.78	39 254	6/8	10	57/56	1.44	Secreted	Lipid transport	R.SAELTASR.L; R.SAELTASR.L
1150	P00505	Aspartate aminotransferase	9.14	47 886	5/11	12	59/56	1.8	Mitochondrion	Fatty acid transport	R.DDNGKPYVLPSVR.K; R.IGASFLQR.F
1964	Q96HG5	β-Actin	5.29	42 052	7/18	20	68/56	1.46	Cytoplasm	Cytoskeleton	K.QEYDESGPSIVHR.K; K.QEYDESGPSIVHR.K
1300	Q9BV35	Calcium-binding mitochondrial carrier protein SCaMC-3	6.85	52 573	11/27	16	73/56	−1.55	Mitochondrion	Transport	R.GLYRGIAPNFMK.V;R.GLYRGIAPNFMK.V
391	Q86WG3	Caytaxin	4.54	46 625	5/6	6	63/56	2.86	Mitochondrion	Transport	M.GTTEATLR.M; R.MENVDVK.E
1998	Q8NI59	E3 ubiquitin-protein ligase MIB2	8.81	111 638	9/11	10	68/56	2.07	Cytoplasm	Protein degradation	R.LQAGHGEWTDDMAPALGR.V;K.CIRCQVVVS
2041	P09382	Galectin-1	5.34	15 048	4/6	29	59/56	1.67	Secreted	Cell growth	K.DSNNLCLHFNPR.F;K.DGGAWGTEQR.E
1134	P46439	Glutathione S-transferase Mu 5	6.9	25 829	5/9	23	57/56	1.45	Cytoplasm	Redox regulation	R.SQWLNEKFK.L;K.CLDAFLNLKDFISR.F
180	P46439	Glutathione S-transferase Mu 5	6.9	25 829	7/13	23	64/56	1.68	Cytoplasm	Redox regulation	R.LCYDPDFEKLKPK.Y; K.CLDAFLNLKDFISR.F
1279	P04406	Glyceraldehyde-3-phosphate dehydrogenase	8.57	36 201	5/9	17	70/56	1.34	Cytoplasm	Glycolysis	K.VGVNGFGR.I;K.LVINGNPITIFQER.D
1270	P04406	Glyceraldehyde-3-phosphate dehydrogenase	8.57	36 201	5/13	20	65/56	1.44	Cytoplasm	Glycolysis	R.VIISAPSADAPMFVMGVNHEK.Y;K.LTGMAFR.V
355	Q96EZ5	Glycosyltransferase 25 family member 3	5.7	67 890	5/7	9	60/56	1.34	Endoplasmic reticulum	Cell adhesion	R.VVDAVDGWMLNSSAIR.N;R.HQFLMELK.Q
309	P11021	Heat shock 70 kDa protein 5	5.07	72 402	13/22	27	98/56	1.92	Endoplasmic reticulum	Protein folding	R.VEIIANDQGNR.I; K.ITITNDQNR.L
308	P11021	Heat shock 70 kDa protein 5	5.07	72 402	18/23	27	150/56	2.27	Endoplasmic reticulum	Protein folding	R.IINEPTAAAIAYGLDKR.E; K.VTHAVVTVPAYFNDAQR.Q
224	Q9UC56	Heat shock 70 kDa protein 9	5.87	73 920	6/9	9	64/56	1.42	Endoplasmic reticulum	Protein folding	K.SDIGEVILVGGMTR.M; K.SDIGEVILVGGMTR.M
185	P11142	Heat shock cognate 71 kDa protein	5.37	71 082	8/19	15	80/56	2.42	Endoplasmic reticulum	Protein folding	R.FEELNADLFR.G; K.SQIHDIVLVGGSTR.I
1330	Q9UC36	Heat shock protein β-1	5.98	22 826	5/11	23	73/56	1.49	Cytoplasm	Protein folding	R.GPSWDPFR.D;R.DWYPHSR.L
1440	Q9UD42	Inducible NO synthase	8.2	132 573	8/12	6	66/56	1.4	Cytoplasm	Redox regulation	R.FDVVPLVLQANGR.D;R.FCAFAHDIDQK.L
617	P07476	Involucrin	4.62	68 851	4/6	9	57/56	1.37	Cytoplasm	Cytoskeleton	R.EMEENFAVEAANYQDTIGR.L; K.MALDIEIATYR.K
1044	O96033	Molybdopterin synthase sulfur carrier subunit	4.36	9806	3/5	30	59/56	1.4	Cytoplasm	Biosynthesis	R.SETISVPQEIK.A; K.SAEITGVR.S
304	P30304	M-phase inducer phosphatase 1	6.49	59 734	7/15	9	59/56	1.37	Nucleus	Cell cycle	R.MLSSNER.D;K.ESTNPEK.A
1505	Q8NFW8	N-acylneuraminate cytidylyltransferase	8.16	49 033	8/5	8	57/56	1.34	Nucleus	Biosynthesis	R.WSEIQK.G;K.GAATSVSNPR.G
2039	P35398	Nuclear receptor ROR-alpha	5.97	64 306	6/8	8	59/56	2.33	Nucleus	Gene regulation	R.CQHCR.L;R.MQQQQR.D
1164	Q8WUD1	Ras-related protein Rab-2B	7.68	24 427	5/17	29	70/56	1.39	Plasma membrane	Protein trafficking	MTYAYLFKYIIIGDTGVGK.S; R.GAAGALLVYDITRR.E
1312	Q6ZS82	Regulator of G-protein signaling 9-binding protein	6.84	25 474	4/5	18	57/56	1.3	Plasma membrane	Signal transduction	K.ALAAILFGAVLLAAVALAVCVAK.L; M.AREECK.A
1090	Q52LW3	Rho GTPase-activating protein 29	6.32	143 514	6/8	5	65/56	1.3	Cytoplasm	Signal transduction	R.EILAQLR.T;K.HLNSSQPSGFGPANSLEDVVR.L

Table 2 *(continued)*

No.	Swiss-prot No.	Protein name	p*I*	M_w	No. match. peptides	Cov. (%)	Score	25 mM/5.5 M (Cys/lys)[a]	Subcellular location	Functional ontology	Match peptide sequences
1820	P57772	Selenocysteine-specific elongation factor	8.61	65 890	5/5	10	62/56	1.48	Cytoplasm	Biosynthesis	R.LAFHGILLHGLEDR.N; K.AGQATEGHCPR.Q
2012	P51817	Serine/threonine-protein kinase	6.36	41 041	6/12	18	58/56	1.95	Cytoplasm	Cell signaling	K.VMSIPDVIR.L;M.EAPGLAQAAAAESDSRK.V
1349	O75461	Transcription factor E2F6	5.35	31 996	4/8	15	56/56	1.5	Nucleus	Cell cycle	M.SQQRPAR.K;K.DCAQQLFELTDDK.E
1935	Q01995	Transgelin	8.87	22 653	4/10	18	58/56	1.55	Cytoplasm	Cytoskeleton	K.HVIGLQMGSNR.G;K.DMAAVQR.T
904	P60174	Triosephosphate isomerase	6.45	26 938	9/20	42	95/56	1.8	Cytoplasm	Glycolysis	K.VVLAYEPVWAIGTGK.T
1081	P11441	Ubiquitin-like protein 4A	8.71	17 823	4/6	26	56/56	5.33	Cytoplasm	Protein degradation	K.LNVPVRQQR.L;R.LASRFLHPEVTETMEK.G

[a] Average fold-differences of triplicate samples run on different gels from DeCyder analysis show labeling changes on free thiol group of cysteine residues for ARPE-19 cells maintained in 25 mM glucose *versus* in 5.5 mM glucose. In here, ICy5 signals were used to monitor cysteine-labeling alterations against ICy3 signals used as internal standard, followed by normalized with protein expression changes. NHS-Cy2 was used to label lysine residues on proteins (to monitor protein expression changes) and was used to normalize ICy3 signals used as internal standard.

Fig. 9 Distribution of differential ICy-labeled proteins between 25 mM glucose and 5.5 mM glucose incubated ARPE-19 cells according to (A) subcellular location and (B) biological function. The classification of the biological functions and sub-cellular locations of these identified proteins are based on a Swiss-Prot search and KEGG pathway analysis.

concentration-induced redox-modulated proteins identified in this study.[51] Defective Rho GTPase-activating protein might, therefore, influence the morphology of retinal pigment epithelium cells and mediate their detachment. Similarly, galectin-1 is reportedly involved in retinal cell adhesion to the photoreceptor through interaction with β-galactoside residue-containing glycoconjugates in the interphotoreceptor matrix.[52] High glucose concentration-induced ROS might modulate galectin-1 activity through the redox modification of its cysteine residues. Impaired galectin-1 might then disrupt the adhesion of retinal cells, leading to serious retinopathy such as macular edema.

The retinoid X receptor (RXR) belongs to a family of nuclear receptors that are activated by retinoic acid and play important roles as ligand-driven transcription factors in fundamental biological processes such as glucose homeostasis. The RXR can form functional heterodimers with several other nuclear receptors such as the retinoic acid receptor and the vitamin D receptor.[53] Singh *et al.* identified that oxidative stress/JNK signaling mediates high glucose concentration-induced suppression of the RXR/retinoic acid receptor complex in cardiomyocytes.[54] Reducing oxidative stress can restore RAR/RXR signaling and protect cardiomyocytes from hyperglycemia.[55] In a mouse model, RXR maintained the normal function and survival of retinal pigmented epithelium cells and prevented loss of viability by shortening and disorganizing their outer segments and reducing light responses.[56] Our data indicated that high glucose concentrations down-regulated

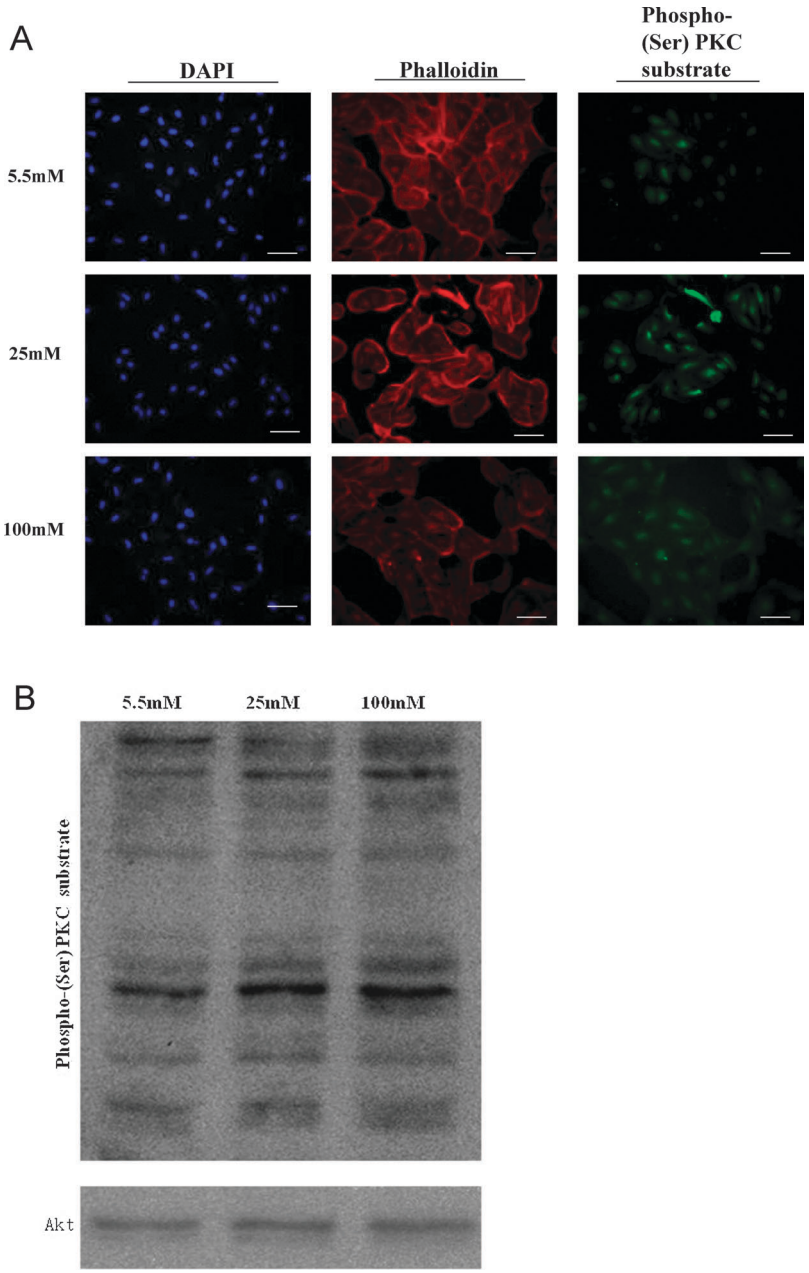

Fig. 10 Immunofluorescence and immunoblotting analysis of the activation of Phospho-(Ser) PKC substrates for ARPE-19 cells incubated in 5.5 mM, 25 mM and 100 mM glucose. (A) ARPE-19 cells incubated in 5.5 mM, 25 mM and 100 mM glucose for at least 3 weeks on cover slips were fixed and stained with Phospho-(Ser) PKC substrates, Phalloidin and DAPI. Each set of fields were taken using the same exposure, and images are representative of 6 different fields. Scale bar = 50 μm. (B) ARPE-19 cell lysates from the same growth conditions were immunoblotted with *anti*-Phospho-(Ser) PKC substrates antibody.

RXR expression in human retinal pigmented epithelium cells and, in turn, might suppress RAR/RXR signaling and the interactions between RXR and other nuclear receptors. Accordingly, high glucose attenuates the protective ability of RXR and reduces the cell viability of retinal epithelial cells against hyperglycemia.

Glyceraldehyde-3-phosphate dehydrogenase (GAPDH) is a tetramer that catalyzes a key reaction in the glycolytic pathway. It is also one of the critical redox-sensitive proteins that has an active cysteine sulfhydryl site and is susceptible to ROS.[57–61] Our redox-proteomics results indicated that high glucose concentration-induced ROS indeed contribute to the redox-modification of GAPDH and, in turn, block the glycolytic pathways. Thus, high glucose-induced oxidative stress can redirect carbohydrate fluxes to generate increased reducing power in the form of NADPH through the pentose phosphate pathway at the expense of glycolysis.

The four proteins (lamin B2, PUMA, WTAP and ASGR1) identified by immunoblotting and one protein (prohibitin 2) identified by ELISA have shown differential expression in clinical plasma, suggesting that these proteins are potential disease markers for diabetic retinopathy (Fig. 6). Importantly, all of

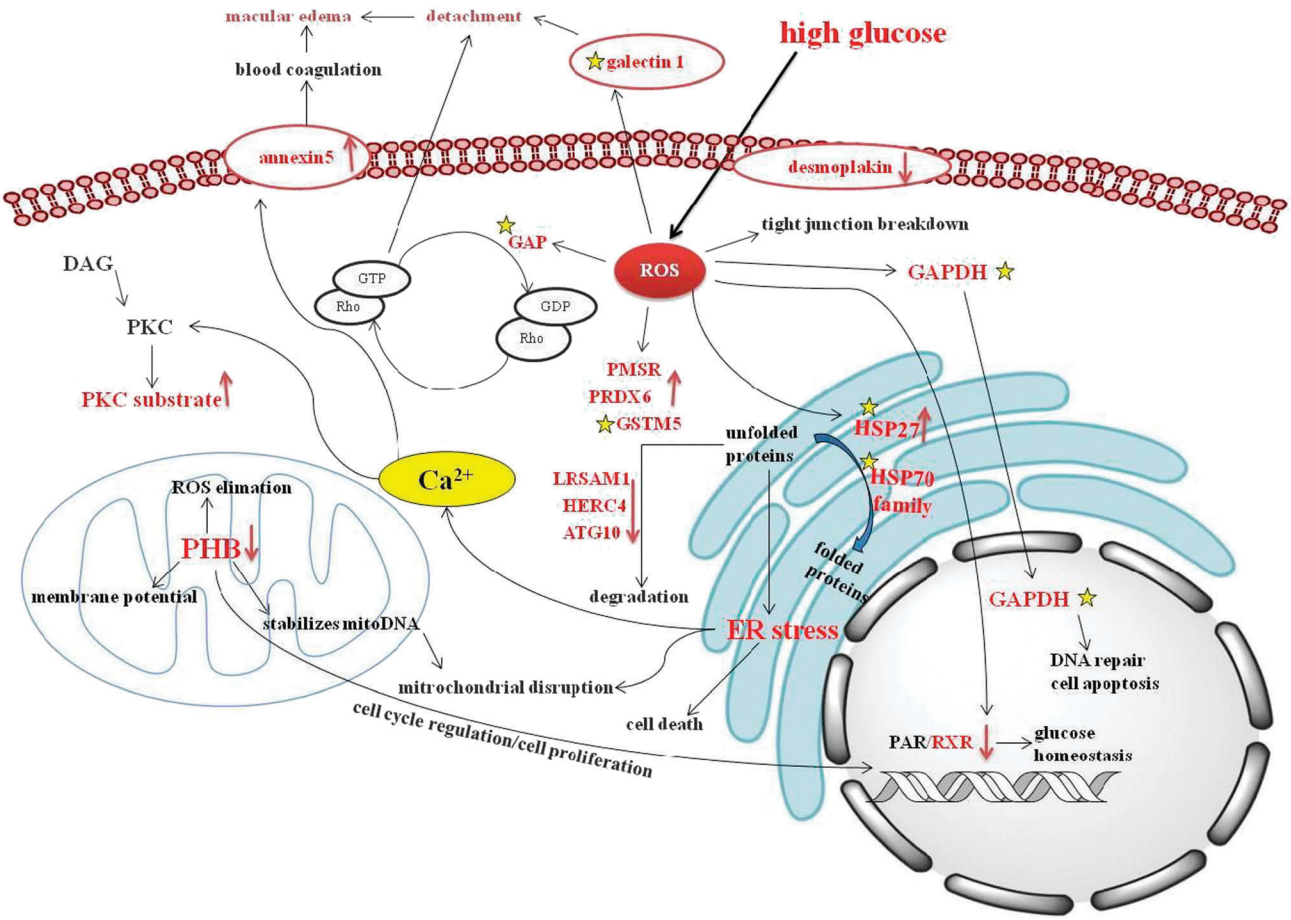

Fig. 11 The hypothetical mechanisms of high glucose-induced differential protein expression and redox-modification in ARPE-19 cells.

these proteins have not been reported as markers for diabetic retinopathy, further implying that these proteins might not only be evaluated as disease markers for the disease, but elucidate the detail mechanisms in diabetic retinopathy-associated regulations. Further investigation shows that the combinations of these identified proteins have not yet been described as markers for other diseases. Accordingly, the combination of these identified proteins could be evaluated as diabetic retinopathy specific markers.

In summary, in this study, we performed comprehensive proteomic analysis of retinal pigmented epithelium cells cultured in various concentrations of glucose. We identified differentially expressed proteins, and developed a novel redox proteomic strategy for monitoring redox-modulated proteins in retinal ARPE-19 cells, following their treatment with high glucose concentrations. We identified high glucose concentration-modulated proteins that participate in several cellular responses including metabolism, cell apoptosis, signal transduction, gene regulation and transport. Our study results indicated the presence of an entire network of proteins in retinal cells exposed to high glucose concentrations, which might play roles in the development of diabetic retinopathy (Fig. 11). Comparison of plasma specimens from type 2 diabetic retinopathy patients with those from healthy donors confirmed the changes in expression of 5 proteins (lamin B2, PUMA, WTAP, AGPR1, and prohibitin 2) in diabetic retinopathy. Our findings indicate potential markers of diabetic retinopathy that are suitable for early-stage evaluation of disease prognosis. The identified proteins might also represent potential targets for treatment of hyperglycemia-induced retinopathy.

Declaration of competing interests

The authors confirm that there are no conflicts of interest.

Abbreviations

1-DE	one-dimensional gel electrophoresis
2-DE	two-dimensional gel electrophoresis
Ab	antibody
CCB	colloidal coomassie blue
CHAPS	3-[(3-cholamidopropyl)-dimethylammonio]-1-propanesulfonate)
ddH_2O	double deionized water
DIGE	differential gel electrophoresis
DTT	dithiothreitol
FCS	fetal calf serum
IP-WB	immunoprecipitation-immunoblotting
MALDI-TOF MS	matrix assisted laser desorption ionization-time of flight mass spectrometry

NP-40	Nonidet P-40
ROS	reactive oxygen species
RSH	free thiol group
TFA	trifluoroacetic acid

Acknowledgements

This work was supported by NSC grant (100-2311-B-007-005) from National Science Council, Taiwan, and toward world-class university project (100N2051E1), NTHU Booster grant (99N2908E1) and Nano- and Micro-ElectroMechanical Systems-based Frontier Research on Cancer Mechanism, Diagnosis, and Treatment grant from National Tsing Hua University, Taiwan.

References

1 H. Dorchy and D. Toussaint, *Rev. Med. Brux.*, 1984, **5**, 319–331.
2 D. M. van Reyk, M. C. Gillies and M. J. Davies, *Redox Rep.*, 2003, **8**, 187–192.
3 A. W. Stitt, *Invest. Ophthalmol. Visual Sci.*, 2010, **51**, 4867–4874.
4 F. Gelisken and F. Ziemssen, *Ophthalmologe*, 2010, **107**, 773–786.
5 R. Ehrlich, A. Harris, T. A. Ciulla, N. Kheradiya, D. M. Winston and B. Wirostko, *Acta Ophthalmol.*, 2010, **88**, 279–291.
6 T. N. Crawford, D. V. Alfaro, III, J. B. Kerrison and E. P. Jablon, *Curr. Diabetes Rev.*, 2009, **5**, 8–13.
7 A. Girach and H. Lund-Andersen, *Int. J. Clin. Pract.*, 2007, **61**, 88–97.
8 P. Gillery, *Ann. Biol. Clin.*, 2006, **64**, 309–314.
9 S. F. Yan, R. Ramasamy and A. M. Schmidt, *J. Mol. Med.*, 2009, **87**, 235–247.
10 E. Boulanger, J. L. Wautier, P. Dequiedt and A. M. Schmidt, *Nephrol. Ther.*, 2006, **2**(Suppl 1), S8–S16.
11 H. Vlassara, *Diabetes Metab. Res. Rev.*, 2001, **17**, 436–443.
12 H. Zill, R. Gunther, H. F. Erbersdobler, U. R. Folsch and V. Faist, *Biochem. Biophys. Res. Commun.*, 2001, **288**, 1108–1111.
13 H. Yang, X. Jin, L. C. Wai Kei and S. K. Yan, *Clin. Chem. Lab Med.*, 2011, **49**, 1773–1782.
14 F. Q. Schafer and G. R. Buettner, *Free Radic. Biol. Med.*, 2001, **30**, 1191–1212.
15 J. C. Lim, H. I. Choi, Y. S. Park, H. W. Nam, H. A. Woo, K. S. Kwon, Y. S. Kim, S. G. Rhee, K. Kim and H. Z. Chae, *J. Biol. Chem.*, 2008, **283**, 28873–28880.
16 C. Jacob, A. L. Holme and F. H. Fry, *Org. Biomol. Chem.*, 2004, **2**, 1953–1956.
17 B. R. Herbert, J. L. Harry, N. H. Packer, A. A. Gooley, S. K. Pedersen and K. L. Williams, *Trends Biotechnol.*, 2001, **19**, 3–9.
18 T. Rabilloud, *Electrophoresis*, 1994, **15**, 278–82.
19 P. H. Hung, Y. W. Chen, K. C. Cheng, H. C. Chou, P. C. Lyu, Y. C. Lu, Y. R. Lee, C. T. Wu and H. L. Chan, *Mol. BioSyst.*, 2011, **7**, 1990–1998.
20 H. L. Huang, H. W. Hsing, T. C. Lai, Y. W. Chen, T. R. Lee, H. T. Chan, P. C. Lyu, C. L. Wu, Y. C. Lu, S. T. Lin, C. W. Lin, C. H. Lai, H. T. Chang, H. C. Chou and H. L. Chan, *J. Biomed. Sci.*, 2010, **17**, 36.
21 T. C. Lai, H. C. Chou, Y. W. Chen, T. R. Lee, H. T. Chan, H. H. Shen, W. T. Lee, S. T. Lin, Y. C. Lu, C. L. Wu and H. L. Chan, *J. Proteome Res.*, 2010, **9**, 1302–1322.
22 Y. W. Chen, H. C. Chou, P. C. Lyu, H. S. Yin, F. L. Huang, W. S. Chang, C. Y. Fan, I. F. Tu, T. C. Lai, S. T. Lin, Y. C. Lu, C. L. Wu, S. H. Huang and H. L. Chan, *Funct. Integr. Genomics*, 2011, **11**, 225–239.
23 H. C. Chou, Y. W. Chen, T. R. Lee, F. S. Wu, H. T. Chan, P. C. Lyu, J. F. Timms and H. L. Chan, *Free Radic. Biol. Med.*, 2010, **49**, 96–108.
24 H. C. Chou, Y. C. Lu, C. S. Cheng, Y. W. Chen, P. C. Lyu, C. W. Lin, J. F. Timms and H. L. Chan, *J. Proteomics*, 2012, **75**, 3158–3176.
25 C. L. Wu, H. C. Chou, C. S. Cheng, J. M. Li, S. T. Lin, Y. W. Chen and H. L. Chan, *J. Proteomics*, 2012, **75**, 1991–2014.
26 H. L. Chan, P. R. Gaffney, M. D. Waterfield, H. Anderle, M. H. Peter, H. P. Schwarz, P. L. Turecek and J. F. Timms, *FEBS Lett.*, 2006, **580**, 3229–3236.
27 H. L. Chan, S. Gharbi, P. R. Gaffney, R. Cramer, M. D. Waterfield and J. F. Timms, *Proteomics*, 2005, **5**, 2908–2926.
28 H. Candiloros, S. Muller, N. Zeghari, M. Donner, P. Drouin and O. Ziegler, *Diabetes Care*, 1995, **18**, 549–551.
29 S. H. Saydah, M. Miret, J. Sung, C. Varas, D. Gause and F. L. Brancati, *Diabetes Care*, 2001, **24**, 1397–1402.
30 X. Jouven, R. N. Lemaitre, T. D. Rea, N. Sotoodehnia, J. P. Empana and D. S. Siscovick, *Eur. Heart J.*, 2005, **26**, 2142–2147.
31 L. Cai, W. Li, G. Wang, L. Guo, Y. Jiang and Y. J. Kang, *Diabetes*, 2002, **51**, 1938–1948.
32 P. Ghezzi, V. Bonetto and M. Fratelli, *Antioxid. Redox Signaling*, 2005, **7**, 964–972.
33 M. Rohde, M. Daugaard, M. H. Jensen, K. Helin, J. Nylandsted and M. Jaattela, *Genes Dev.*, 2005, **19**, 570–582.
34 F. Barutta, S. Pinach, S. Giunti, F. Vittone, J. M. Forbes, R. Chiarle, M. Arnstein, P. C. Perin, G. Camussi, M. E. Cooper and G. Gruden, *Am. J. Physiol. Renal Physiol.*, 2008, **295**, F1817–F1824.
35 K. Mori, *Tanpakushitsu Kakusan Koso*, 1999, **44**, 2442–2448.
36 A. A. Sadighi Akha, J. M. Harper, A. B. Salmon, B. A. Schroeder, H. M. Tyra, D. T. Rutkowski and R. A. Miller, *J. Biol. Chem.*, 2011, **286**, 30344–30351.
37 K. Kitiphongspattana, C. E. Mathews, E. H. Leiter and H. R. Gaskins, *J. Biol. Chem.*, 2005, **280**, 15727–15734.
38 K. Nakamura, E. Bossy-Wetzel, K. Burns, M. P. Fadel, M. Lozyk, I. S. Goping, M. Opas, R. C. Bleackley, D. R. Green and M. Michalak, *J. Cell Biol.*, 2000, **150**, 731–740.
39 Y. Akita, *J. Biochem.*, 2002, **132**, 847–852.
40 Z. Naor, S. Shacham, D. Harris, R. Seger and N. Reiss, *Cell Mol. Neurobiol.*, 1995, **15**, 527–544.
41 Y. Ye, *Essays Biochem.*, 2005, **41**, 99–112.
42 C. Osman, C. Merkwirth and T. Langer, *J. Cell Sci.*, 2009, **122**, 3823–3830.
43 C. Merkwirth and T. Langer, *Biochim. Biophys. Acta*, 2009, **1793**, 27–32.
44 M. Schleicher, B. R. Shepherd, Y. Suarez, C. Fernandez-Hernando, J. Yu, Y. Pan, L. M. Acevedo, G. S. Shadel and W. C. Sessa, *J. Cell Biol.*, 2008, **180**, 101–112.
45 A. M. Czarnecka, C. Campanella, G. Zummo and F. Cappello, *Cancer Biol. Ther.*, 2006, **5**, 714–720.
46 E. K. Han, T. Mcgonigal, C. Butler, V. L. Giranda and Y. Luo, *Anticancer Res.*, 2008, **28**, 957–963.
47 J. C. Zech, I. Pouvreau, A. Cotinet, O. Goureau, B. Le Varlet and Y. de Kozak, *Invest. Ophthalmol. Visual Sci.*, 1998, **39**, 1600–1608.
48 E. C. Leal, A. Manivannan, K. Hosoya, T. Terasaki, J. Cunha-Vaz, A. F. Ambrosio and J. V. Forrester, *Invest. Ophthalmol. Visual Sci.*, 2007, **48**, 5257–5265.
49 J. Lee, M. Ko and C. K. Joo, *J. Cell Physiol.*, 2008, **216**, 520–526.
50 Y. Zheng, H. Bando, Y. Ikuno, Y. Oshima, M. Sawa, M. Ohji and Y. Tano, *Invest. Ophthalmol. Visual Sci.*, 2004, **45**, 668–674.
51 S. Y. Moon and Y. Zheng, *Trends Cell Biol.*, 2003, **13**, 13–22.
52 F. Uehara, N. Ohba and M. Ozawa, *Invest. Ophthalmol. Visual Sci.*, 2001, **42**, 2164–2172.
53 G. Allenby, M. T. Bocquel, M. Saunders, S. Kazmer, J. Speck, M. Rosenberger, A. Lovey, P. Kastner, J. F. Grippo and P. Chambon, *Proc. Natl. Acad. Sci. U. S. A.*, 1993, **90**, 30–34.
54 A. B. Singh, R. S. Guleria, I. T. Nizamutdinova, K. M. Baker and J. Pan, *J. Cell Physiol.*, 2011, **227**, 2632–2644.
55 R. S. Guleria, R. Choudhary, T. Tanaka, K. M. Baker and J. Pan, *J. Cell Physiol.*, 2011, **226**, 1292–1307.
56 M. Mori, D. Metzger, S. Picaud, C. Hindelang, M. Simonutti, J. Sahel, P. Chambon and M. Mark, *Am. J. Pathol.*, 2004, **164**, 701–710.
57 S. Azam, N. Jouvet, A. Jilani, R. Vongsamphanh, X. Yang, S. Yang and D. Ramotar, *J. Biol. Chem.*, 2008, **283**, 30632–30641.
58 A. E. Brodie and D. J. Reed, *Arch. Biochem. Biophys.*, 1990, **276**, 212–218.
59 R. C. Cumming, N. L. Andon, P. A. Haynes, M. Park, W. H. Fischer and D. Schubert, *J. Biol. Chem.*, 2004, **279**, 21749–21758.
60 L. Zheng, R. G. Roeder and Y. Luo, *Cell*, 2003, **114**, 255–266.
61 Z. Dastoor and J. L. Dreyer, *J. Cell Sci.*, 2001, **114**, 1643–1653.